Quaternary International xxx (xxxx) xxx

Contents lists available at ScienceDirect

Quaternary International

journal homepage: www.elsevier.com/locate/quaint

Investigating Holocene relative sea-level changes and coastal dynamics in the mid-Tyrrhenian coast, Italy: An interdisciplinary study

C. Caporizzo [a], A. Gionta [b], G. Mattei [b,*], M. Vacchi [c], G. Aiello [d], D. Barra [d], R. Parisi [e], G. Corrado [f], G. Pappone [b], P.P.C. Aucelli [b]

[a] Department of Engineering, Università Telematica Pegaso, Centro Direzionale, Isola F2, 80143, Naples, Italy
[b] Department of Science and Technology, Università degli Studi di Napoli "Parthenope", Centro Direzionale, Isola C4, 80143, Naples, Italy
[c] Department of Earth Sciences, Università di Pisa, Via Santa Maria, 53, 56126, Pisa, Italy
[d] Department of Earth Sciences, Environment and Resources, University of Naples Federico II, Via Cinthia, 21, 80126, Naples, Italy
[e] Italian National Research Council, Piazzale Aldo Moro, 7, 00185, Rome, Italy
[f] Department of European and Mediterranean Cultures, Environment, and Cultural Heritage, University of Basilicata, Via Lanera, 20, 75100, Matera, Italy

ARTICLE INFO

Keywords:
Coastal geomorphology
Landscape evolution
Sea-level proxy
Isostatic adjustment
Mid-tyrrhenian sea

ABSTRACT

Understanding millennial changes in relative sea level (RSL) and coastal responses in stable regions is crucial for deciphering the intricate relationship between natural dynamics and human adaptation. This interdisciplinary study explores the interplay between mid-to-Late Holocene sea-level fluctuations and tectonic along the mid-Tyrrhenian coast.

The study area, located between the Fondi and Garigliano coastal plains, held great significance in ancient times. In particular, the strategic role of Formia, a monitoring point for the Tyrrhenian Sea, made this city one of the most important commercial hub during Roman occupation, leading to a significant urbanization of the coastal stretch testified by well-preserved remains nowadays scattered along the submerged or semi-submerged coastal sectors.

This study reconstructs the mid-to-Late Holocene morpho-evolution and RSL changes in the study area by creating a geodatabase made of 52 sea-level markers (SLMs) derived from direct geoarchaeological measurements, stratigraphic and palaeoecological interpretations of new borehole data, and previously published stratigraphic data. Specifically, the radiocarbon dating of three peat samples provided new data ranging between 7.62 ± 47 and 1.00 ± 51 ka BP on the sea level history in the area. Based on our dataset, between 9.0 and 8.0 ka BP, the sea level rose from −19 m to −6.5 m at a rate of about 15.6 mm/y, slowing to 0.8 mm/y afterwards, stabilizing at its current position. Results suggest that during the 1st century BC, local sea level was no higher than −0.55 ± 0.29 m.

The collected RSL data support the hypothesis of tectonic stability of this sector during the last 2.0 ka, testified by the position of the SLMs in accordance with the glacio-hydro-isostatic adjustment (GIA) models and supported by the determination of average vertical ground movement rates of −0.017 ± 0.23 mm/y.

Finally, in terms of coastal changes the overlay between new data from geoarchaeological surveys, reinterpretation of previously-published stratigraphic data, and geomorphological analysis allowed us to deduce a general coastal progradation trend in the historical time for both low-lying and rocky sectors, due to natural and anthropogenic forcing factors.

1. Introduction

Coastal environments are among the most dynamic and complex landscapes on our planet, whose evolution is the result of a variety of geological and climatic forcings (e.g., Adloff et al., 2015; Corrado et al., 2018, 2020; Aucelli et al., 2022; Georgiou et al., 2022; Karymbalis et al., 2022). The interplay of these forces has resulted in a constantly evolving coastal morphology, presenting unique challenges and opportunities for scientific understanding and management. Geological processes such as tectonic activity and sedimentation, coupled with climatic drivers such

* Corresponding author.
E-mail address: gaia.mattei@uniparthenope.it (G. Mattei).

https://doi.org/10.1016/j.quaint.2024.08.009
Received 16 March 2024; Received in revised form 26 July 2024; Accepted 27 August 2024

as sea-level fluctuations and storm activity, contribute to the dynamic nature of coastal regions (e.g., Budillon et al., 2022a; Amato et al., 2018). Additionally, human activities, including urbanization, exert significant pressures on coastal ecosystems, notably in the Mediterranean areas (e.g., Kaniewski et al., 2013; Anthony et al., 2014; Caporizzo et al., 2021a, 2021b, 2024; Mattei et al., 2023), exacerbating the existing natural variability.

Understanding the complex interactions between these factors is crucial for predicting and mitigating the impacts of coastal change, ensuring the resilience and sustainability of these vital ecosystems (e.g., Mattei et al., 2022a, 2024; Martínez-Sánchez et al., 2023; Tursi et al., 2023).

In particular, the coastal sector stretching between the Fondi and Garigliano coastal plains (mid-Tyrrhenian Sea, central Mediterranean), has been the subject in the past of several geological studies focused on its morphological and environmental evolution, sometimes outdated or mainly referring to research spatially limited to narrow sectors of the coastal strip (Ozer et al., 1987; Antonioli et al., 1988; Antonioli, 1991; Abate et al., 1998; Devoti et al., 2004; Aiello et al., 2007, 2021; De Pippo et al., 2007; Bellotti et al., 2016; Doorenbosch and Field, 2019; van Gorp and Sevink, 2019; Sevink, 2020; Sevink et al., 2020, 2021; Di Lorenzo et al., 2021; Corrado et al., 2022).

The set of previously published data available so far, sometimes divergent from each other and characterized by a limited areal distribution, on one hand needs to be revised in the light of new knowledge, and on the other fails to give a sufficiently coherent picture regarding the behaviour of this area during the Holocene.

In light of these considerations, a study was needed to bring together the different coastal features of this area in order to homogenize the data on its evolution through the search for a set of indicators capable of shedding light on the Holocene evolution of the area, so far completely insufficient and lacking in correlation between different proxies located over the different sectors.

In this research, we untangle the mid-to-Late Holocene coastal evolution of Central-Southern Tyrrhenian coastal sectors (central Mediterranean Sea), in order to reconstruct the interplay between sea-level fluctuations and tectonics in this sector of the Mediterranean region by putting together a dataset of relative sea-level (RSL) data.

In particular, we carried out a multidisciplinary approach made of geomorphological and geoarchaeological analysis coupled with new biostratigraphical data to quantitatively define the different factors that controlled the recent coastal evolution, aiming to identify any possible presence of Holocene tectonic influence on the regional sea-level changes. In fact, vertical displacements (VD) play an important role in

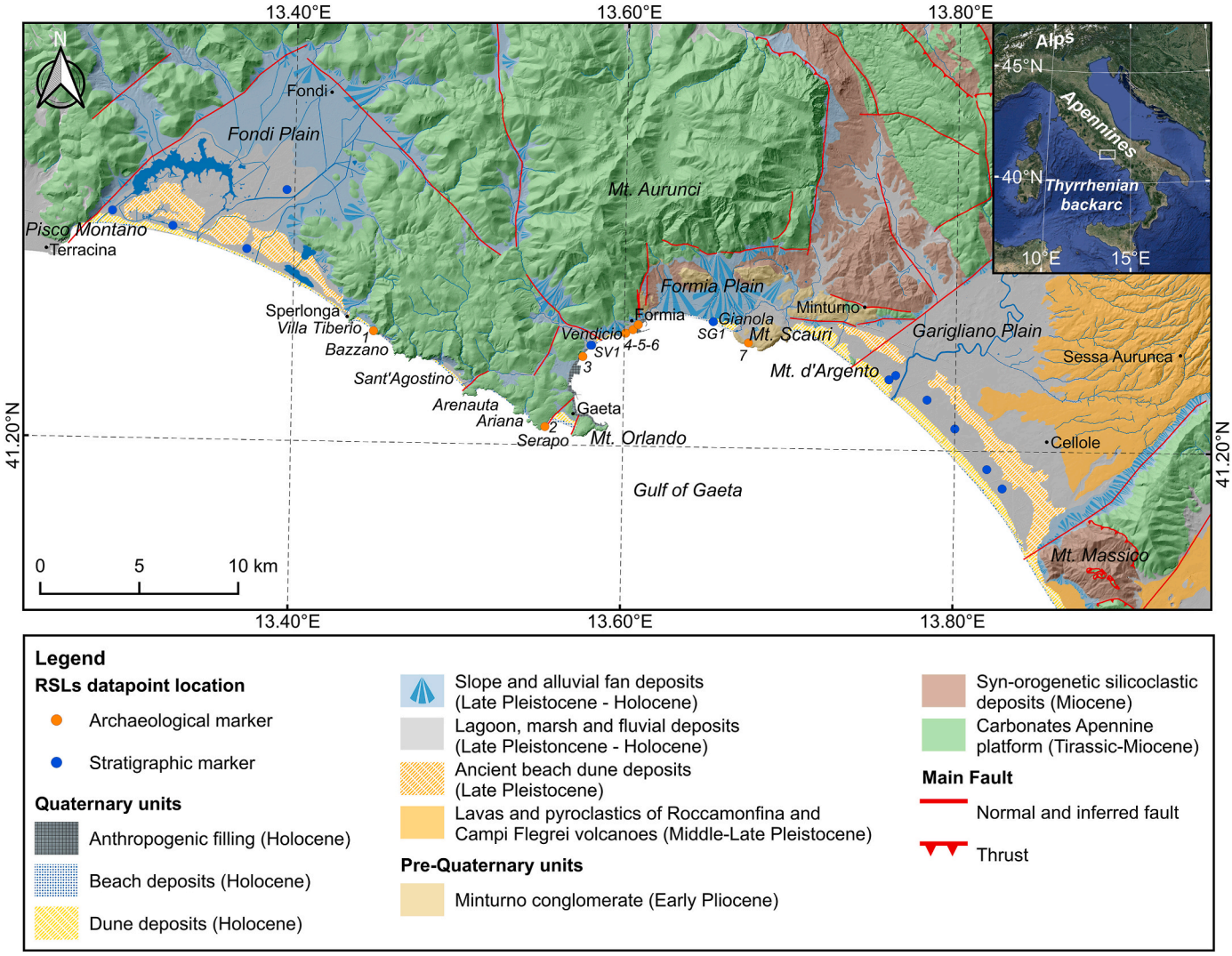

Fig. 1. Simplified geological sketch of the study area with position of RSLs datapoint and archaeological site (Villa Tiberio, Geo Fonteo, Villa Accetta, Villa Rubino, Marina di Castellone, Sarinola - Formia Harbour, and Porticciolo di Gianola, respectively from 1 to 7). Units and faults modified from: Antonioli et al., 1988; Acocella and Funiciello (2006); Milia et al. (2013); Smeraglia et al. (2019); van Gorp and Sevink (2019); Aiello et al. (2021); Tavani et al. (2021); Corrado et al. (2022).

local sea-level changes and coastal variations (e.g., Scicchitano et al., 2011; Vacchi et al., 2020; Budillon et al., 2022b; Mattei et al., 2022b).

Therefore, along the coastal sector, a robust assessment of VDs is mandatory to define current and future coastal vulnerability. Much of the mid and southern Tyrrhenian Sea was affected by significant tectonic activity during the Quaternary (e.g., Acocella and Funiciello, 2006; Milia et al., 2013; Conti et al., 2017; Smeraglia et al., 2019; Tavani et al., 2021).

This work represents the first cluster of data aimed at analyzing the mid-to-Late Holocene evolution of the coastal sector considering mainly the relative sea-level fluctuations, leaving the door open for further creation of specific morphoevolutive models.

2. Geological and geomorphological setting

The study area extends approximately 90 km, stretching from the Pisco Montano promontory in Terracina in the northwest to Monte Massino in Sessa Aurunca in the southeast (Fig. 1). This region is part of one of the most representative coastal segments along the central-southern Tyrrhenian margin of the Apennine chain (e.g., Antonioli et al., 1988; Antonioli, 1991; De Pippo et al., 2007; Aiello et al., 2021; Corrado et al., 2022).

In a short stretch of coastline, various features and landforms reveal a complex framework resulting from Quaternary normal block faulting (Corrado et al., 2022). Due to this complex geological evolution, this coastal sector is characterized by alternating NE-SW trending carbonate ridges (green unit in Fig. 1) such as Pisco Montano and Mt. Massico, and structural depressions such as Fondi Plain, Formia Plain, and Garigliano Plain, filled mainly by thousand-meter successions of clastic and partly by pyroclastic-volcanic products (light orange unit in Fig. 1; e.g., Ippolito et al., 1973; Antonioli et al., 1988; Billi et al., 1997; Acocella and Funiciello, 2006; Cosentino et al., 2006; Iannace et al., 2013; Milia et al., 2013, 2017; Tavani et al., 2021). The NE-SW-striking faults are responsible for the articulation evolution of the coast between Sperlonga and Gaeta. These faults are responsible for the alternation of sandy pocket beaches and Mesozoic limestone headlands (green unit in Fig. 1), as can be seen in the beach systems of Villa Tiberio, Bazzano, Sant'Agostino, Arenauta, Ariana and Serapo, separated by small promontories such as Torre Truglia, Villa Tiberio, Torre Capovento, Torre San Vito, Torre Scissura, Torre Viola and Mt. Orlando.

In the northern sector, the Fondi plain is a rhomboidal structural depression bounded by NE-SW and NW-SE striking main faults (Acocella and Funiciello, 2006) (Fig. 1). The area is characterized by a system of deeply incised Late Pleistocene beach ridges and associated inland lagoons, partially filled with lagoonal clays (respectively orange grid and grey units in Fig. 1; Antonioli et al., 1988; Devoti et al., 2004; van Gorp and Sevink, 2019). The inland part of this lagoonal plain is covered by colluvial fan deposits (green banded unit in Fig. 1) due to land-use-related soil erosion that began in early Roman times or earlier (Attema, 2017). Around 4000 years ago, a slowdown in sea-level rise (Lambeck et al., 2011; Vacchi et al., 2016) led to the formation of late-Holocene narrow beach ridges and lagoons, infilled with peat over marine sands and characterized of presence of two distal tephra from Campanian volcanoes, presumably ascribable to Astroni 6 eruption from the Campi Flegrei area and Avellino EU5 from the Vesuvian eruption (Doorenbosch and Field, 2019; van Gorp and Sevink, 2019; Sevink et al., 2020, 2021).

Moving southeast, the coastal area between Sperlonga and Gaeta is composed of Mesozoic limestone and characterized by rocky cliffs (green unit in Fig. 1; Budillon et al., 2020, 2022). Talus deposits, composed of carbonate breccias with a matrix texture supported by reddish sand-clay, develop at the foot of several slopes, such as the eastern side of the Sant'Agostino plain. These formations typically overlie Mesozoic limestone and are attributed to the last glacial period (e.g., Antonioli, 1991; De Pippo et al., 2007). Along NE-SW-trending tectonic lineaments, several embayments formed, where sandy deposits accumulated since the Middle Pleistocene (Corrado et al., 2020, 2022).

In the western sector of Formia plain, the Pontone River flows. It is the most representative torrential watercourse of the area and its valley in the upper branch is rather deep and NW-SE oriented, following the trend of the faults bounding the graben in which it flows (Fig. 1; Corrado et al., 2022). The lower branch of Pontone River flows through a small coastal plain near Vendicio, the uppermost part of which is filled with a 20 m thick transitional sequence of marsh to lagoonal sediments, followed by littoral and finally continental deposits (Aiello et al., 2007). The Vendicio coastal plain is a narrow strip of coast that stretches about 2 km from Monte Conca in the West to Marina di Castellone in the East (Fig. 1). The area is mainly characterized by a sandy beach, with pebbles found locally at the mouth of the Pontone River. Behind the modern dune ridge, which was completely dismantled and urbanized, there is a NW-SE oriented paleocliff (Aiello et al., 2007).

Southeast of the Formia plain, a small coastal plain called Gianola stretches up to the promontory of Monte di Scauri (Fig. 1; Corrado et al., 2022). This coastal plain is characterized by alluvial fan deposits (light blue banded unit in Fig. 1) interdigitated with other Quaternary deposits, such as the lagoonal clays (grey unit in Fig. 1) and fine sands with peats and pyroclastics, and the aeolian red sands (Corrado et al., 2022).

Recently, the Formia coastal sector has become more stable. However, coastal dynamics continue to cause beach erosion, more evident in the eastern sector of the study area, where a series of breakwaters were constructed to protect the Formia coastline for over 4 km (Valente, 2010). The main cause of the erosive process is the interruption of the sediment transport by the harbour piers, which is associated with a drastic decrease in the sediment load of the small basins towards the southern foothills of the Aurunci Mts.

In the southern sector of the study area, the Garigliano coastal plain has a squared shape with sides of about 12 km, bounded by NE-SW striking main faults (Fig. 1; Bergomi et al., 1969; Ippolito et al., 1973; Aiello et al., 2021). Quaternary units in this area include marine coastal deposits, silty marsh deposits (grey unit in Fig. 1), and pyroclastic products from Roccamonfina and Campi Flegrei (orange unit in Fig. 1). The outcrop units are represented by dune deposits dated at Upper Pleistocene (Brancaccio et al., 1990) and Holocene dunes (respectively orange and yellow grid units in Fig. 1), which extend roughly parallel to the coast. The innermost dune is located 2–3 km back from the current coast and is mainly composed of weathered aeolian sands. Below these sands, a half-meter thick fossiliferous, coarse-grained calcarenite was dated through the Amino Acid Racemisation (AAR) technique at about 130,000 years ago (Brancaccio et al., 1990), indicating RSL was at about 6 m Medium Sea Level (MSL; Mattei et al., 2022b). Recently 230 Th/U dating performed on some bioconstruction occurring in correspondence with the tidal notch in Mt. Argento indicates the RSL dropped at about 1.6 m MSL at the end of the LIG (~86 ka) (Mattei et al., 2022b). The rest Holocene facies, on the other hand, are only known from well logs (Abate et al., 1998; Bellotti et al., 2016; Aiello et al., 2021; Di Lorenzo et al., 2021).

3. Archaeological setting

The study area experienced significant anthropic modifications since the Roman era (e.g., last 2 millennia). Indeed, several Roman archaeological structures are scattered along the coastal area, particularly associated with aristocratic villas from the 1st century BC. These structures include fish tanks and coastal defense structures, found in locations such as Villa Tiberio, Gneo Fonteo, Villa Accetta, Villa Rubino, Marina di Castellone, Sarinola (Formia Harbour), and Porticciolo di Gianola (refer to Fig. 1 for their specific locations).

The research area is located within the historical *Sinus Formianus*, a coastal region covering the entire length of the Gulf, encompassing present-day Formia, Gaeta, Itri, and part of Sperlonga (Traina, 2000). During Roman times, Formia played a strategic role for Rome in terms of

monitoring the Tyrrhenian Sea, and it was appreciated both as a commercial pole and as a pleasant holiday destination, second only to Baia, also known for its thermal baths.

The city's origins are sparsely documented, with a common belief suggesting Greek origins, supported by the ancient Greek name of *Hormiai* or *Phormiai*. According to Strabo, the toponym originated from "*hormos*" (i.e. port or landing place), indicating the coastal features existing when the initial Spartan settlers arrived (Traina, 2000).

In 338 BCE, during the Roman period, *Formiae* attained *municipium* status, receiving from Rome "citizenship without the right to vote" (Traina, 2000). At the same time, a *praefectus* (i.e. delegate of the praetor of Rome) was established, reflecting a cohabitation system between local magistracies and direct Roman control. This favoured economic expansion by enhancing maritime trade routes, coupled with accelerated connections to Rome facilitated by the construction of the Via Appia. In 188 BCE, the municipalities of Formia, Fondi, and Arpino effectively became integral parts of the Roman Republic (Livio, 38, 36, 7–9), experiencing substantial urban development.

Towards the conclusion of the Republican era, the Gulf of Formia's coast, distinguished by favourable climatic conditions and scenic beauty, saw the construction of numerous maritime villas. These properties were owned by affluent and influential figures of the time, featuring distinctive structures and environments such as fishponds and nymphaea (Cassieri, 2015).

Similar to the coastal region of Baia in Campania, the coastal stretch between Formia and Gaeta underwent significant urbanization during this period. Remnants of this urbanization persist today, visible in submerged, semi-submerged, or partially submerged coastal structures along the current shoreline, characterized by remarkably well-preserved conditions.

4. Methods

A multi-proxy approach has been used to reconstruct the mid-to-Late Holocene RSL and associated coastal changes in the study area. We produced a suite of sea-level data points derived from the reinterpretation of previously published data, new archaeological sea-level markers, and bio-stratigraphic analysis of cores performed in the coastal plains of Formia (Fig. 1). We further coupled this new dataset with the sea-level data extracted from the available database (Mattei and Vacchi, 2023).

The selection of archaeological sites for surveying was based on a thorough examination of bibliographic, cartographic, and video-graphic materials providing descriptions and dating for the ruins. Special emphasis was placed on identifying ancient piscinae (fish tanks), recognized as highly accurate sea-level markers within the context of Roman coastal structures, as highlighted by previous studies (e.g., Leoni and Dai Pra, 1997; Lambeck et al., 2004; Evelpidou et al., 2012; Vacchi et al., 2016).

The stratigraphic unpublished dataset was made available for study by public institutions. The new two deep boreholes were drilled in 2023 in Formia Plains.

4.1. Geo-archaeological surveys

We performed on-land and underwater surveys in order to measure the structural elements of the archaeological remains, including Roman fish tanks and coastal defence structures as *pilae* (i.e., cubic concrete structures utilized as pillars for piers or coastal constructions).

Measurements at the study sites had a vertical accuracy error ranging from ±1 to ±5 cm, depending on the type of used tool. The 3D position of the archaeological elements was measured employing a GPS antenna (Emlid Reach RS2) with a GPS/RTK data acquisition (accuracy of ±3 cm) mounted on a graduated range pole, by correcting the vertical measurements with respect to the local geoid referred to the mean sea level. In the case of underwater measurements, where the submerged elements were located at a depth of more than 1 m, the depth measurements were carried out under optimal meteo-marine conditions with centimetric accuracy by using a metric staff. In this case, the detected measurements were corrected with respect to the hydrometric level at the time of the survey taken from the mareographic station in the Port of Gaeta belonging to the National Mareographic Network (ISPRA), to obtain measurements with respect to the mean sea level.

4.2. Stratigraphic analysis

In Formia, the two cores have been analyzed by using a bio-sedimentary approach including analysis of grain size composition, sedimentary structures and macrofossil content. In addition, some selected layers were sampled for further laboratory investigations, including paleoecology analysis (ostracod and foraminiferal assemblages), and ^{14}C AMS dating.

The core SG1, with a depth of 10 m, is located on the nowadays beach in Gianola Plain (13°39′13.84″ E, 41°15′26.41″ N, WGS84 coordinate system). The core SV1, with a depth of 15 m, is located in Vendicio Plain (13°34′48.11″ E, 41°14′44.58″ N, WGS84 coordinate system), at the mouth of the Pontone River (see location in Fig. 1).

4.3. Palaeoecological analysis

Analysis was performed on 25 samples (100 g dry weight), 20 collected in Gianola Plain from the core SG1 (depth range: 0.60–9.85 m), and five in the Vendicio Plain from the core SV1 (depth range: 7.15–13.00 m). The samples were dried, disaggregated in boiling water with sodium carbonate, and washed through 230 and 120 mesh sieves (63 and 125 μm); then, the residue was examined under a reflected light binocular microscope.

Carbonaceous plant debris, seeds, radiolarians, sponge spicules, echinoderm spines, and mollusk remains (bivalves, gastropods) have been reported as semi quantitative data (Appendix B).

Benthic foraminiferal tests and ostracod shells were picked from the coarsest fraction (>125 μm).

The number of foraminiferal specimens, the ostracod Minimum Number of Individuals (MNI), and the ostracod Total Number of Valves (TNV) were used for quantitative analysis. MNI consists of the greater number between right and left adult valves plus the number of adult carapaces. When only juvenile shells were recorded, the MNI equals one. TNV includes all the juvenile and adult valves.

Benthic foraminiferal and ostracod taxa were identified according to classic and modern literature both for benthic foraminifers and for ostracods (Meisch, 2000; Aiello and Barra, 2010; Fuhrmann, 2012; Milker and Schmiedl, 2012; Aiello et al., 2018 and references therein).

4.4. Sea-level markers

The sea-level data identified in the study area were categorized into sea-level index points (SLIPs) and terrestrial limiting points (TLPs, which constrain upper limits of paleo RSL positions), following the international protocols for sea-level studies (Shennan and Horton, 2002; Shennan et al., 2015; Khan et al., 2019).

A SLIP is a sea-level marker with a clearly defined relationship between the marker itself and the former sea level (Shennan et al., 2015; Vacchi et al., 2016). According to Shennan et al. (2015), each SLIP has an associated Indicative Meaning (IM).

The IM is made of two parameters: (1) indicative range (IR), representing the elevation range over which the marker formed; and (2) reference water level (RWL), denoting the midpoint of the aforementioned range (Shennan et al., 2015; Vacchi et al., 2016).

Therefore, the determination of the RSL (SLIP) can be evaluated by using the following equation:

$$RSL = A - IR/2 = A - RWL$$

where "A" is the proxy elevation.

Also, SLIPs (Table 1) were generated for the geological samples in our database, following the protocols developed for the Mediterranean region (Rovere et al., 2016; Vacchi et al., 2016) and widely adopted in recent studies (e.g., Brisset et al., 2018; Stocchi et al., 2018; Karkani et al., 2019; Mattei et al., 2022b). Geological samples that do not have a direct association with a previous tidal level can still be interpreted as sea-level limiting points (Table 1).

In this study, numerous archaeological maritime structures were interpreted as SLIPs (Table 1), such as the top of the sluice gate of fish tanks or the concrete change of *pilae*. Consequently, a specific minimum elevation above the MSL at the time of construction was considered for each structure, from now on defined as functional clearance (FC), and considered in the correction of the submersion measurements together with the hydrometric level.

In the case of the fishtank, we attributed the top of the sluice gate (i.e. the vertical post constituting the gate of the tank in which the sliding grooves were carved) a FC of 0.2 m above the former MSL (Aucelli et al., 2021; Mattei et al., 2022; 2024). In the case of the coastal defense structure known as *pilae*, we allocated to the concrete change (i.e. limit between the areas in hydraulic concrete and the areas in concrete totally laid in a subaerial environment; *sensu* Mattei et al., 2018; Aucelli et al., 2020) a FC of 0.5 m (Mattei et al., 2018; Aucelli et al., 2020).

Each data was stored in a standardized geodatabase (SeaProxy, *sensu* Mattei et al., 2022) where we specified age, dating methods and corrections as well as vertical measurements and errors. The total vertical error (or vertical uncertainty, u) was calculated as follows (Vacchi et al., 2016):

$$u_n=(u_{12} + u_{22} + \ldots. + un_2)\ 1/2$$

Where u_n are the sources of error for each SLIP, related to: simple thickness; measuring of the absolute elevation of the indicator; IR uncertainty, intended as the half of the IR (Vacchi et al., 2016).

4.5. Dating methods

The chronology of the RSL data was determined using radiocarbon dating and by the archaeological age of the marine structures (Schmiedt, 1972; Ciccone, 1992, 1995, 2000; Leoni and Dai Pra, 1997).

Radiocarbon dating was performed on two samples from the SV1 borehole and three samples from the SG1 borehole, using the high-resolution mass spectrometry technique (AMS) at the Vilnius Radiocarbon Laboratory - Center for Physical Sciences and Technology (FTMC). The dated material was constituted by organic matter and seeds; therefore, to provide dates in sidereal years with a 2σ range, the radiocarbon ages were calibrated by using CALIB 8.2 (Stuiver and Reimer, 1993) and applying the IntCal 20 dataset.

The chronological constraints derived from bibliographic data were also recalibrated through the analogous procedure by using the same program, employing the IntCal20 (Reimer et al., 2020) and Marine 20 (Heaton et al., 2020) datasets for respectively terrestrial samples and marine samples. In order to account for the reservoir effect in marine samples, a ΔR of −104 ± 39 yr (Mattei and Vacchi, 2023) was applied.

4.6. Statistical analysis

The bibliographic RSL data and the new measurements were combined to produce a new suite of RSL data using a wide range of proxies and following the most recent scientific protocols (Hijma et al., 2015; Khan et al., 2019).

We applied to the new set of SLIPs the Errors in Variables Integrated Gaussian Process (EIV IGP) Model, which performs the Bayesian inference on historical rates of sea level (Cahill et al., 2015). The EIV IGP model, providing the mean of the likelihood for the observed data, captures the continuous and dynamic evolution of sea-level change with

Table 1
The indicative meanings employed for assessing the relative elevation of sea-level index points and database limiting points. HAT - Highest Astronomical Tide; MSL - Medium Sea Level; MHW - Mean High Water, average of all the high water heights; MLW - Mean Low Water, Average of all the low water heights (Shennan et al., 2015).

Sample type	Evidence	Reference water level	Indicative range
SLIPs			
Open lagoon	Foraminiferal and ostracod assemblages are dominated by marine-littoral and brackish taxa, such as *Ammonia aberdoveyensis* (frequently cited as *A. parkinsoniana* and *A. tepida*), *Ammonia beccarii*, *Haynesina depressula* (frequently cited as *Nonion depressulum*), *Haynesina germanica* (frequemtly cited as *Nonion pauciloculum*), *Quinqueloculina* spp., *Aurila* spp., *Cyprideis torosa*, *Loxoconcha elliptica*, *Leptocythere* spp. and *Xestoleberis* spp. (e.g., Mazzini et al., 1999; Carboni et al., 2002; Aiello and Barra, 2010; Rossi et al., 2011; Aiello et al., 2018 and references therein). The macrofossil taxa are mainly dominated by marine-brackish mollusks with the presence of *Cerastoderma glaucum*, *Bittium reticulatum* often associated with *Loripes lacteus*, *Loripes lucinalis*, and *Abra segmentum* (e.g., Gravina et al., 1989; Carboni et al., 2010; Di Rita et al., 2011; Bellotti et al., 2016)). The species diversity is higher compared to the semi-enclosed lagoon system.	−1 m	MSL to −2 m
Semi enclosed lagoon	Foraminiferal and ostracod assemblages characterized by brackish littoral or inner estuarine taxa, such as *Ammonia aberdoveyensis* (in particular "lobate form", v. Aiello et al. (2018), frequently cited as *A. tepida*), *Elphidium granosum* (= *Porosononion granosum* and *Protelphidium granosum*), *Haynesina depressula* (= *Nonion depressulum*), *Haynesina germanica* (= *Nonion pauciloculum*), *Cyprideis torosa, Cytherois fischeri, Leptocythere lagunae*, *Loxoconcha elliptica* (e.g., Amorosi et al., 2009, 2013; Aiello and Barra, 2010; Carboni et al., 2010; Marco-Barba et al., 2013; Aiello et al., 2018 and references therein). Macrofossil taxa mainly represented by brackish molluscs, typical of sheltered marine/lacustrine environments, with the	−0.5 m	MSL to −1 m

(*continued on next page*)

Table 1 (*continued*)

Sample type	Evidence	Reference water level	Indicative range
	occurrence of *Cerastoderma glaucum*, *Abra segmentum* and *Ecrobia ventrosa* (e.g., Caldara et al., 2008; Carboni et al., 2010; Bellotti et al., 2016). The species diversity is lower compared to the open lagoon system.		
Undifferentiated brackish environment	Foraminifer and ostracod mixed (sensu Fagerstrom, 1964) assemblages dominated by freshwater - slightly brackish or marsh taxa and shallow marine taxa, such as *Ammonia aberdoveyensis* (frequently cited as *A. parkinsoniana* and *A. tepida*), *Haynesina germanica* (= *Nonion pauciloculum*), *Candona neglecta, Cyclocypris ovum, Cyprideis torosa, Darwinula stevensoni, Ilyocypris bradyi, Loxoconcha stellifera, Pseudocandona sarsi* (e.g., Carboni et al., 2002; Serandrei-Barbero et al., 2006; Amorosi et al., 2009, 2013; Aiello and Barra, 2010; Aiello et al., 2018 and references therein). Macrofossil taxa mainly represented by *Cerastoderma glaucum*, *Abra segmentum*, *Acroloxus lacustris*, *Bithynia tentaculate*, *Stagnicola palustris* and *Valvata piscinalis* (e.g., Carboni et al., 2010; Bellotti et al., 2016). Presence of swamp plant macrofossil assemblages (e.g., Silvestri et al., 2005; Di Rita et al., 2010).	(HAT to MLW)/2	HAT to MLW
Shoreface	Low-diversity foraminiferal assemblages mainly consisting of poorly preserved specimens, suggesting high energy environment, of the genera *Ammonia* and *Elphidium* (e.g., Amorosi et al., 2013; Aiello et al., 2018 and references therein). Macrofossil taxa mainly represented by *Tellina fabuloides*, *Loripes lacteus* and *Bittium* spp. (e.g., Carboni et al., 2010).	MSL	1 to −1
Concrete change on *pila*	Limit between the areas in hydraulic concrete and the areas in concrete totally laid in a subaerial environment. A functional clearance (FC) of about 0.5 m is supposed for this structural element and considered within the calculation of the RSL (Mattei et al., 2018, 2023b, 2023a, 2024; Aucelli et al., 2020, 2021).	MSL	MHW to MLW
Sluice gate of fish tank	Gate of the tank always built above MHW. A functional clearance (FC) of about 0.2 m is supposed for this structural element and considered within the calculation of the RSL (Mattei et al., 2018, 2023b, 2023a, 2024; Aucelli et al., 2020, 2021).	MSL	MHW to MLW
Lower crepido of fish tank	Walkaway border surrounding the tank. Among the different *crepido* levels, the lower one was always built above MHW. A functional clearance (FC) of about 0.2 m is supposed for this structural element and considered within the calculation of the RSL (Mattei et al., 2018, 2023b, 2023a, 2024; Aucelli et al., 2020, 2021).	MSL	MHW to MLW
Limiting points			
Terrestrial limiting	Ostracod assemblages consisting of species characteristic of continental, non-marine waters dominated by taxa pertaining to the superfamily *Cypridoidea* (e.g., Carboni et al., 2002; Aiello and Barra, 2010, 2011; Rossi et al., 2011; Milli et al., 2013). Macrofossil taxa mainly represented by *Bithynia leachi*, *Bithynia tentaculate*, *Gyraulus laevis*, *Planorbis*, *Valvata cristata* (e.g., Carboni et al., 2010; Bellotti et al., 2016)). Additionally, freshwater plant macrofossils and peat (Colombaroli et al., 2007; Di Rita et al., 2010). Upper beach deposits and terrestrial paleosoils.	MSL	Above MSL

full consideration of all available sources of uncertainty. When two SLIPs of coeval age were placed at different elevations, we only considered the highest one for the statistical reconstruction (Horton and Shennan, 2009; Vacchi et al., 2021).

The Glacio-hydro-isostatic Adjustments (GIA) are commonly explained using the sea-level equation (SLE, Farrell and Clark, 1976). This equation allows for the computation of relative sea-level changes, driven by the mass variations of continental ice sheets and influenced by the response of the Earth's mantle (Farrell and Clark, 1976; Spada and Stocchi, 2007; Milne and Mitrovica, 2008).

Mattei et al. (2022b) computed a series of 54 GIA predictions for the Mid-Tyrrhenian Sea by solving the SLE and incorporating three ice sheet chronologies along with solid Earth rheological models (Mattei et al., 2022b and references therein). In particular, were inferred three values of lithosphere thickness, respectively of 60 km, 90 km, and 120 km, and three ranges of values for the lower and intermediate mantle viscosity between 2 and 10, 0.5–1, and 0.2–0.5 Pa. In this context, the solid Earth is assumed to be spherically symmetric, self-gravitating, rotating, radially stratified, and characterized by linear Maxwell viscoelastic layers.

For the reconstruction of the local RSL history and the differentiation between RSL changes influenced by GIA and those associated with possible local Vertical Displacements (VDs), the acquired RSL data from the online geodatabase were compared with the GIA models.

For each sea-level marker, a Python 3.7 script employing a Bayesian Statistical method based on Monte Carlo simulations was used to compute all potential VD values. This well-established statistical sampling method, widely applied across various scientific disciplines (Eckhardt, 1987), involves generating a set of 'n' random VD values

based on each RSL value. The distribution is displayed on a histogram, with the peak representing the most probable value.

The VD values are algorithmically derived by calculating the difference between observed (RSL_O) and predicted (RSL_P) sea-level positions from the GIA models as follows:

VDn = RSLon - RSLpn

In this context, the value of 'n' is established as 1000.

Moreover, the Python script was also employed to derive the associated subsidence or uplift rates by dividing the 'n' random VD values by the age of the proxy.

5. Results

5.1. Geoarchaeological reconstructions

Seven archaeological sites, located between Sperlonga and Gianola (see Fig. 1 for location), were investigated through geoarchaeological surveys detecting the submersion measurements of particular structural features related to the former RSL.

5.1.1. *Tiberius Villa docks*

The remains of the villa belonging to the Roman emperor Tiberius are located in the southern part of Sperlonga, at the base of a limestone promontory. These remains date back to the end of the Republican Age, around the second half of the 1st century BC. The villa complex included a natural cave, within which a rectangular fish tank was constructed at the beginning of the 1st century BC.

Along the entire coastal stretch in front of the villa, a long row of hydraulic concrete structures is located in semi-submerged environments, which were interpreted as remains of ancient docks. (Fig. 2A; Ciccone, 1995; Leoni and Dai Pra, 1997).

During the direct survey performed at the archaeological site of Tiberius Villa, the submersion measurements of concrete-change level of the ancient dock (*sensu* Mattei et al., 2018), nowadays located at −0.05 m MSL, were measured and corrected with respect to the local hydrometric level. Consequently, the reconstructed RSL related to the second half of the 1st century BC was at −0.55 ± 0.27 m MSL.

5.1.2. *Gneo Fonteo villa pilae*

Along the rocky promontory at the west of Serapo beach in Gaeta, part of the remains of a maritime villa are located in the submerged environment. The villa was attributed to the Roman consul Gneo Fonteo and consequently dated to the second half of the 1st century BC (Schmiedt, 1972; Ciccone, 2000).

At about 17 m from the coastline, a series of five *pilae* occurs (Fig. 2B). These are characterized by a side length of approximately 6 m, constituting the largest side of the structure. The *pilae* are interspersed with channels and connected to the beach by circular walkways that intertwine with each other.

During the direct survey at this site, the submersion measurement of the concrete change of the *pilae*, located at −0.25 m MSL, was measured and corrected with respect to the local hydrometric level. Consequently, the reconstructed RSL related to the second half of the 1st century BC was at −0.75 ± 0.27 m MSL.

5.1.3. *Accetta Villa fish tank*

The remains of the Roman villa of Accetta, dating back to the 1st century BC, are located at Punta Conca, near the narrow Vendicio coastal plain (Ciccone, 2000; Vitiello, 2017). The ancient villa has an upper section, with visible traces at various heights integrated into the modern structure, and a lower section, which hosts the remains of a fish tank in the semi-submerged area. The tank's triangular shape follows the profile of the coastline behind it (Fig. 2C).

During the direct survey of the fish tank, no *in situ* vertical posts of the sluice gate were found. Consequently, after measuring the length of one of the collapsed vertical posts identified at the bottom of the tank, from its base to the top of the vertical post, and correcting the local hydrometric level, it was possible to estimate the submersion measurement of this archaeological feature of −0.12 m MSL, assuming the post was originally in a vertical position. Consequently, the reconstructed RSL related to the 1st century BC was at −0.52 ± 0.27 m MSL.

Fig. 2. – Direct geoachaeological surveys carried out at different sites with the location of the measuring points. A: Tiberius Villa; B: Gneo Fonteo; C: Accetta Villa; D: Rubino Villa; E: Marina di Castello; F: Sarinola; G: Porticcioli di Gianola.

5.1.4. *Rubino Villa fish tank*

In the Caposele archaeological area in Formia, the remains of several Roman *villae* occur close to the present-day touristic harbour. Among those, the remains of a fish tank are located at the foot of the modern constructions of Rubino Villa and are dated by bibliographic sources to the 1st century BC (Ciccone, 2000).

During the direct survey at this site (Fig. 2D), the submersion measurement of the lower *crepido* level was measured at −0.22 m MSL. Consequently, the reconstructed RSL related to the 1st century BC was at −0.62 ± 0.27 m MSL.

5.1.5. *Marina di castellone pilae*

In Marina di Castellone, remains of the Roman port of Formia (Ciccone, 1992; Leoni and Dai Pra, 1997), occur close to the modern port. The remains of this harbour structure, in operation since at least the end of the 2nd century BC, are characterized by the presence of eight submerged concrete *pilae* extending for a curved stretch of approximately 300 m to the south.

During the direct survey at this site, the submersion measurement of the concrete change of one of the *pila* (Fig. 2E), nowadays located at −0.10 m MSL, was measured and corrected with respect to the local hydrometric level. Consequently, the reconstructed RSL related to the end of the 2nd and the beginning of the 1st century BC was at −0.60 ± 0.27 m MSL.

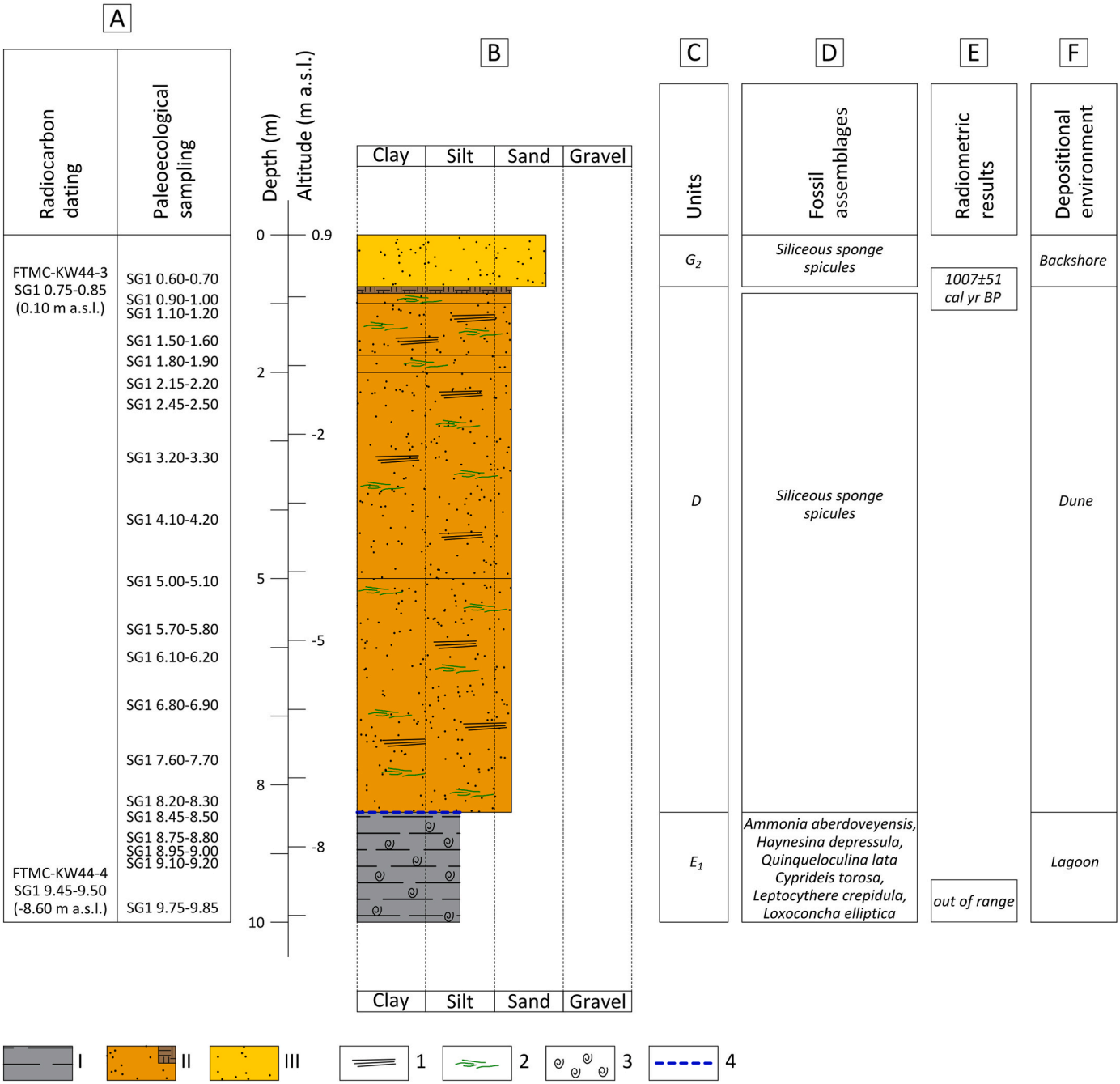

Fig. 3. – Simplified Sedimentological log of the core SG1. Columns show from the left to the right: (A) selected samples used for analyses; (B) log: (I) lagoon deposits, (II) dune deposits and paleosoil, (III) beach sand deposits, (1) lamination, (2) plant remains, (3) fossil, (4) erosional surface; (C) Units; (D) vertical distribution of the meiofaunal assemblages; (E) Radiometric results; (F) Resulting depositional environments, also suggested by vertical evolution of lithofacies.

5.1.6. Sarinola (Formia Harbour) fish tank

The Sarinola fish tank, located in the area of the modern harbour and partially buried in 1950 by the modern coastal road, was part of the maritime villa of the Republican Age dated to the second half of the 1st century BC (Schmiedt, 1972; Leoni and Dai Pra, 1997; Ciccone, 2000).

The fish tank, with a length and a width of respectively 60 and 30 m, has a rectangular shape and is characterized by the presence of 15 inner thanks distributed among the central squared part and the two-lateral rhomboid-shaped sectors.

During the direct survey at this site, the submersion measurement of the top of the sliding grooves of the sluice gate (Fig. 2F), nowadays located at −0.15 m MSL, was measured and corrected with respect to the local hydrometric level. Consequently, the reconstructed RSL related to the second half of the 1st century BC was at −0.55 ± 0.27 m MSL.

5.1.7. Porticciolo di gianola fish tank

Along the promontory of Mt. Scauri (Gianola), the remains of an ancient Roman villa extend over an area of about 12 ha. The villa, built on three different levels, was attributed to Mamurra, a Roman politician originally from Formia, and consequently dated to the 1st century BC (Ciccone, 2000).

The luxurious residence also included a fish tank, built within a natural inlet, that later on was partially dismantled with its materials reused in other constructions (Ciccone, 2000; Pesando and Stefanile, 2015). Only in a few cases, some elements can still be found in their original position, leaving a valuable trace of the location of at least two of the probable inner basins (Pesando and Stefanile, 2015).

During the direct survey at this site, the submersion measurement of the top of the sliding grooves of the sluice gate (Fig. 2G), nowadays located at −0.10 m MSL, was measured and corrected with respect to the local hydrometric level. Consequently, the reconstructed RSL related to the second half of the 1st century BC was at −0.50 ± 0.27 m MSL.

5.2. Stratigraphic analysis

The first core is located at Gianola Beach (SG1), east of Formia, and reaches a depth of 10 m. Three distinct sedimentary units were identified (Fig. 3). The first sedimentary unit (E1) extends from the core base to −7.5 m MSL and consists of grey silty clay with planar horizontal structures and numerous millimetric/centimetric-sized shell remains (among others *Cerastoderma glaucum*, *Abra segmentum*, *Hydrobiidae* sp.).

A distinct erosional surface, whose age is difficult to define, marks the transition to Unit D. The deposit is characterized by fine, well-sorted, yellowish-reddish laminated sands, mainly composed of quartz with minor feldspar and containing common plant remains, and it extends from −7.5 m to 0.10 m MSL. This interval shows a clear transition upwards to a 10-cm-thick paleosoil consisting of brown sandy clay with bioturbations. The upper unit G2 consists of medium-fine, well-sorted yellowish sands primarily composed of quartz, with minor feldspar and lithic fragments.

Among the three samples dated using radiocarbon technique, only one provided a reliable result, dating the top of unit D (Fig. 3; sample KTMC-KW44-3 in Table 2) to 1007 ± 51 cal Yr BP. For unit E1, the remaining two samples are out of range and the carbon dating method was unable to provide a reliable result.

The second borehole was drilled in the Vendicio Plain (SV1), west of Formia, reaching a maximum depth of 15 m. In this core, four distinct sediment units were identified (Fig. 4). The first one (Unit CI), spans from the base of the core to −9.9 m MSL and consists of lightly lithified, light grey volcaniclastic silty sand containing fresh glass fragments.

A distinct erosion surface, marks the transition to unit G1 The sediments between −9.9 m and −3 m MSL are characterized by brown, coarse, silty sand, abundant plant debris, carbonate granules, fragments of ceramics and charcoal, and frequent bioturbation Moreover, this unit exhibits two clear transitions to 1-m-thick and 30-cm-thick levels, consisting of blackish peaty clay that is rich in organic matter and abundant in plant remains. Two samples, FTMC-KW44-1 and FTMC-KW44-2 have been dated using the radiocarbon technique, providing an age of 7494.5 ± 67.5 cal Yr BP and 7622 ± 47 cal Yr BP, respectively (refer to Fig. 4 and Table 2).

The G6 upper unit consists of greyish and yellowish medium-fine sand containing limestone pebbles and occasionally interspersed with greyish silt and sandy silt layers. This suggests a mixed provenance of terrestrial and marine sources, indicative of a transitional coastal environment, such as a littoral or estuarine environment. The core ends with an anthropogenic fill (Unit H) of carbonate cobbles, pebbles, sand, and landfill material resulting from the canalization of the Pontone River in the modern age.

5.2.1. Paleoecology

Nineteen samples were collected from the Core SG1 are fossiliferous; the sample SG1 1.10–1.20 is barren. Meiofaunal assemblages consist of benthic foraminifers, radiolarians, sponge spicules, echinoderm spines, bivalves, gastropods, and ostracods (Appendix B). Benthic foraminiferal assemblages are present in six samples and include eleven species in nine genera. Ostracod assemblages occur in five samples and consist of three species. *Ammonia aberdoveyensis* (benthic foraminifera), and *Cyprideis torosa* (ostracods) are the commonest species. A total of 18149 foraminiferal tests and 76856 ostracod valves have been studied.

Two intervals have been recognized. The lower part of the core includes five samples ranging from 9.85 to 8.45 m. Assemblages are characterized by euryhaline marine species and by taxa typical of marginal-brackish waters. The uppermost interval, including 15 samples, ranging from 8.30 to 0.60 m, shows very poor, mainly siliceous meiofaunal assemblages, suggesting a backshore (emerged) paleoenvironment and/or deposition in low pH waters, where CaCO3 remains are not preserved (Aiello et al., 2018, 2021; and references therein).

One sample out of five samples from the Core SV1 (Vendicio Plain) is barren, the remaining four being fossiliferous. The latter yielded meiofaunal assemblages consisting of carbonaceous plant debris and seeds (Appendix C). On the base of meiofaunal assemblages, Core SV1 succession can be subdivided in two intervals.

- Interval 1: 13.00–12.95 m; the sample is devoid of fossil remains. It represents a level collected within the volcanic deposits, generally barren.
- Interval 2: 9.95–7.15 m; the sediments are characterized by the presence of carbonaceous plant debris and seeds; both calcareous and siliceous meiofossil are lacking. Low pH waters, due to the presence of abundant organic matter, may induce the dissolution of CaCO3 remains. A swampy paleoenvironment can be inferred.

5.3. Holocene sea-level variations

The dataset analyzed in this study is composed of 52 mid-to-Late Holocene RSL data, spanning the central-southern Tyrrhenian coast.

Table 2
Table of new radiocarbon dated samples (latitude and longitude are in WGS84).

Sample	Lab. Code	Location	Latitude	Longitude	Unit	Dated facies	Depth (m)	C14 age (yr BP)	Calibrated age (yr BP)
SV1 7.15–7.2	FTMC-KW44-1	Formia. Vendicio Plain	41.24572	13.58002	G1	Seeds	7.2	6562 ± 34	7494.5 ± 67.5
SV1 9.90–9.95	FTMC-KW44-2	Formia. Vendicio Plain	41.24572	13.58002	G1	Seeds	9.95	6748 ± 34	7622 ± 47
SG1 0.75–0.85	FTMC-KW44-3	Formia. Gianola Plain	41.2572	13.65345	D	Organic matter	0.8	1090 ± 28	1007 ± 51

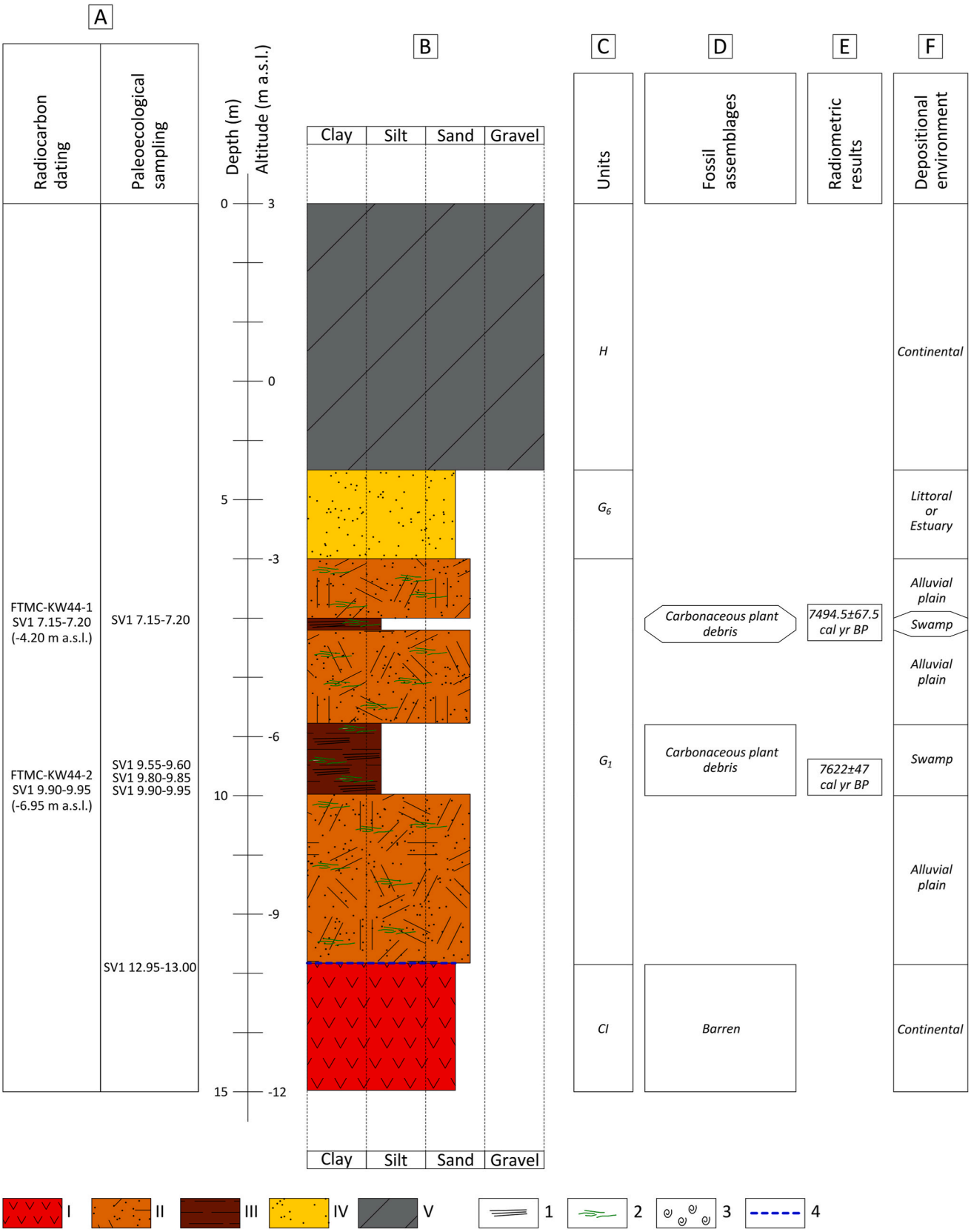

Fig. 4. – Simplified Sedimentological log of the core SV1. Columns show from the left to the right: (A) selected samples used for analyses; (B) log: (I) volcanoclastic deposits, (II) Alluvial deposits, (III) marsh deposits, (IV) fluvial deposits, (V) anthropic deposits, (1) lamination, (2) plant remains, (3) fossil, (4) erosional surface; (C) Units; (D) vertical distribution of the meiofaunal assemblages; (E) Radiometric results; (F) Resulting depositional environments, also suggested by vertical evolution of lithofacies.

The database includes 42 SLIPs and 10 TLPs (sea proxy or Appendix A; Figs. 5 and 6).

In the Fondi plain (light blue dots in Fig. 6), the database consists of 17 SLIPs and 1 TLP from sediment cores. Here, the oldest SLIP, dated 8.67 ± 0.22 ka BP, places the RSL at −18,6 ± 1.1 m and the TLP constrain the RSL below −15.8 ± 0.36 m at 8.15 ± 0.17 ka BP. Late Holocene SLIPs from undifferentiated brackish environment sediments indicate that the RSL ranged between −2.29 ± 0.54 m at 4.06 ± 0.08 ka BP and −2.05 ± 0.54 m at 3.84 ± 0.12 ka BP. In Sperlonga and Gaeta (orange dots in Fig. 6), the database consists of 3 SLIPs derived from the Roman archaeological structures of Villa Tiberio, Gneo Fonteo, and Villa Accetta. These data place the RSL between −0.52 ± 0.27 m and −0.75 ± 0.27 m at 2.0 ± 0.05 ka BP.

In the Formia coastal sector (orange dots in Fig. 6), the database consists of 5 SLIPs and 3 TLPs. A SLIP derived from core data in the Vendicio coastal plain suggests an RSL of −16.1 ± 0.28 m at 8.4 ± 0.2 ka. In the same area, TLPs from new coring indicate that RSL was below −6.95 ± 0.25 m at 7.62 ± 0.04 ka BP and −4.2 ± 0.24 m at 7.49 ± 0.07 ka BP. During the Roman age (2.0 ± 0.05 ka BP), 4 geoarchaeological SLIPs suggest that the RSL ranged between −0.65 ± 0.27 and −0.50 ± 0.27 m. The most recent data include a TLP from paleosoil on top of a dune deposit in a new core from the Gianola Plain, indicating that the RSL was below 0.1 ± 0.23 m at 1.0 ± 0.05 ka BP.

In the Garigliano coastal plain (light and dark green dots in Fig. 6), the database consists of 17 SLIPs and 6 TLPs. Data derived from swamp, salt marsh, and lagoon deposits detected in previously published cores. The data exhibit a slight scatter, likely related to the variability in subsidence rates driven by sediment compaction. However, the SLIPs indicate a consistent rise in RSL during the early-mid Holocene, from −6.55 ± 0.21 m at 8.18 ± 0.15 ka BP to −2.6 ± 0.21 m at 5.04 ± 0.21 ka BP. The younger SLIP suggests RSL was still at −3.5 ± 0.21 m at 4.06 ± 0.16 ka BP. The only representation for other younger data is through TLPs, which did not permit a thorough evaluation of the RSL evolution during the late Holocene period.

6. Discussion

The new suite of sea-level data, combined with previously published data, provides fresh insights into the sea-level evolution in this broad sector of the Tyrrhenian Sea.

The oldest data indicate that, between 9.0 and 8.0 ka BP, the RSL in the area was characterized by rates of RSL rise of 15.6 mm/yr, bringing the RSL from −19 m to −6.5 m in less than 1000 years. In this period, the whole suite of models overestimates the RSL position (Fig. 5) as already observed in other portions of the central and western Mediterranean coast (Vacchi et al., 2018; Mattei et al., 2022b). After 8.0 ka BP, we observed a sudden deceleration with rates lower than 0.8 mm/y. This is consistent with the global decrease of the meltwater input derived from the northern hemisphere ice-sheet (Peltier, 2004; Lambeck et al., 2014).

Since that period, the statistical reconstruction shows a general agreement between data and models. This suggests a general tectonic stability of this broad coastal sector as also confirmed by the VD computed with the Monte Carlo approach. In fact, VD values in the last 8.0 ka BP typically do not exceed ±0.4 mm/y decreasing to ±0.2 mm/y in the last 5.0 ka BP.

Generally, in the low-lying coastal sectors (Fondi and Garigliano coastal plains), we observed a minor subsidence trend which increased from 8.2 ka BP to 3.6 ka BP with the age of the SLIPs (Fig. 7). This subsidence is likely controlled by compaction as already observed in the Volturno plain (Corrado et al., 2018, 2020). The increasing trend from mid to late Holocene can be explained by taking into account that younger sediments are more affected by compaction subsidence than older ones deposited on even older and more compacted materials. In fact, archaeological data in Fondi coastal plain demonstrate a further decrease up to 0.03 mm/yr of this subsidence in the last 2.0 ka BP.

The slightly higher rates measured in the Garigliano plain between 8.18 and 4.07 ka BP are related to the case of a core drilled at the river mouth (indicated in Fig. 7 with a dark green colour), where sedimentary compaction processes are more significant. However, also in this case, the subsidence rates do not exceed the value of ±0.5 mm/y, stated as tectonic stability cutoff (see red box in Fig. 7).

In rocky coastal sectors, archaeological data further testified to overall tectonic stability in the last 2.0 ka BP, with VD values ranging between 0.1 and 0.03 mm/yr.

In terms of coastal changes, a general coastal progradation was reconstructed for both low-lying and rocky sectors, even if due to different forcing factors.

The coastal progradation of about 1 km in 7.3 ka in the Garigliano plain can be attributed to the combined action of sedimentary inputs coming from the Garigliano River and low rates of sea level rise. The

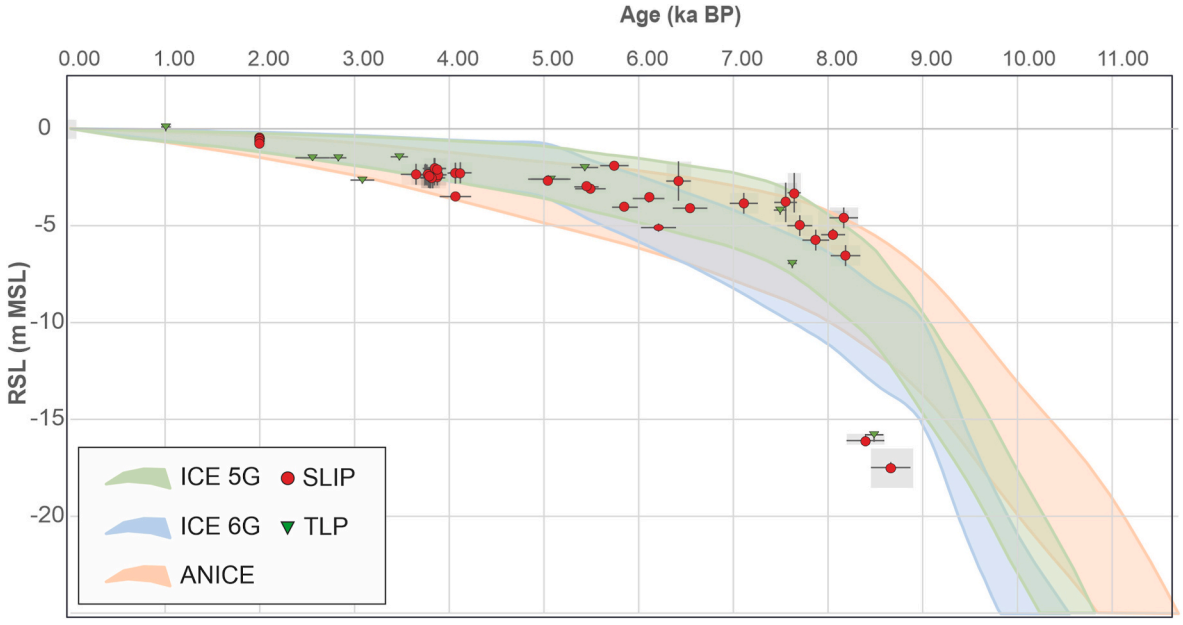

Fig. 5. – New sea-level database of Southern Latium and comparison between the RSL measurements and the GIA models from Mattei et al. (2022).

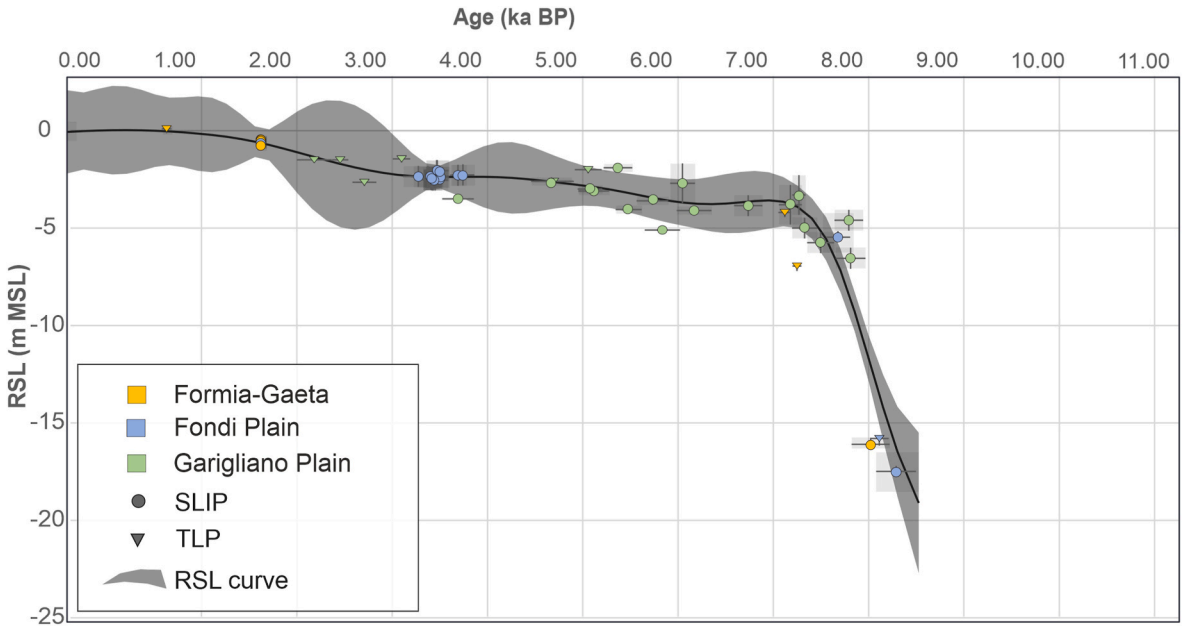

Fig. 6. – The SLMs of the geodatabase and the resulting local RSL curve calculated applying the EIV IGP model (Cahill et al., 2015). Sea-level index points (SLIPs) are represented by circles, while terrestrial limiting points (TLPs) by triangles. The SLMs from the coastal sector between Formia and Gaeta (see Fig. 1 for location) are shown in yellow, those from Fondi coastal plain in light blue, and those from Garigliano coastal plain in green.

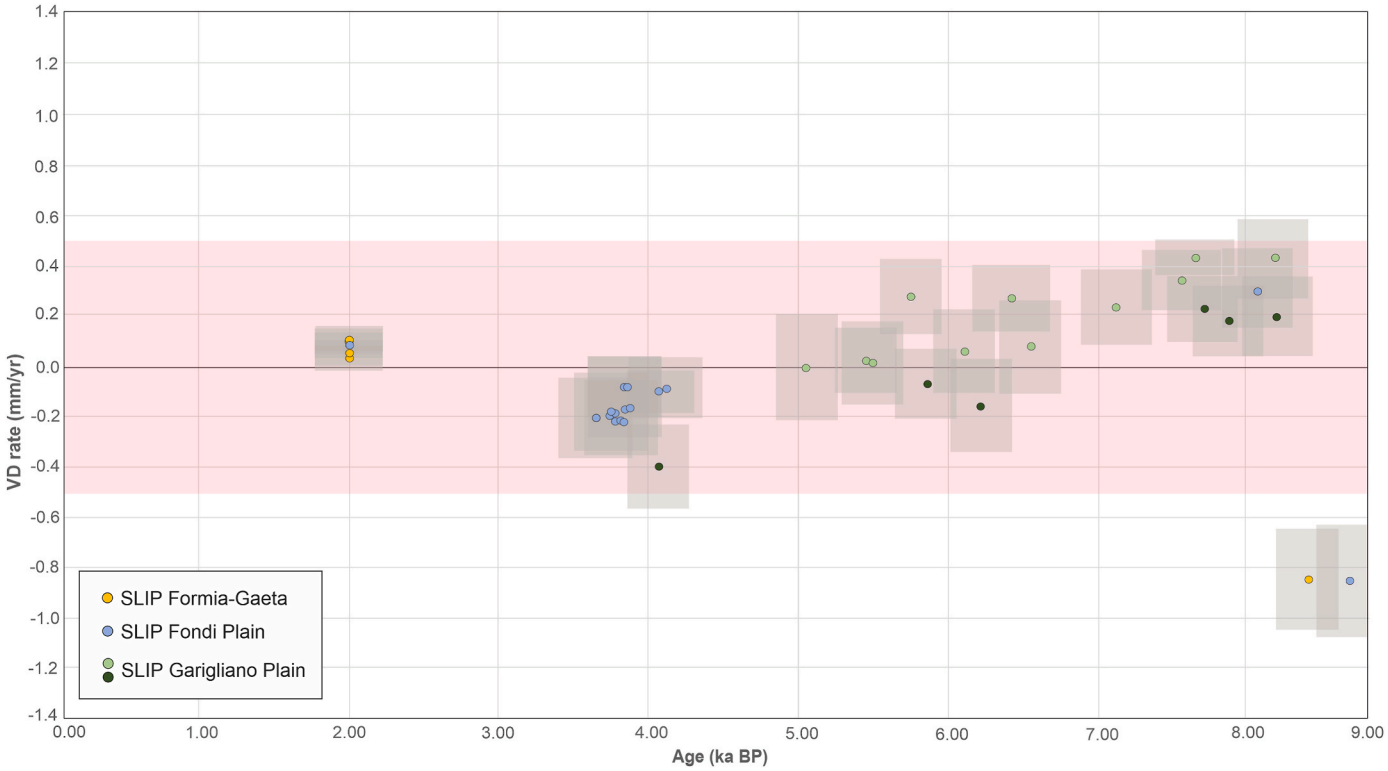

Fig. 7. – Vertical displacement rates (VD rate, in mm/yr) distribution calculated through the Monte Carlo procedure from the SLIPs included in the geodatabase. Each VD was calculated as a difference between the measured (marker) and estimated (GIA) value. The three sectors are differentiated based on the colour: orange for the Formia-Gaeta coastal sector; light blue for the Fondi Plain; green for the Garigliano Plain, where the darker colour is associated with higher subsidence rates observed among same age intervals. The red box represents the tectonic stability cutoff: above and below VD rates ranging from 0.5 and −0.5 mm/yr, the area is no longer considered tectonically stable.

same trend was measured in Fondi Plain, where 5.3 ky-old stratigraphic data positioned the shoreline 500 m inland. However, this progradation ended at about 2.0 ka BP as testified by the position of Tiberio villa and its maritime annexes (Fig. 8b) on the present shoreline.

Besides, within the stratigraphic sequences of core SG1 in Gianola plain, at the west of the Garigliano plain (see Fig. 1 for location), a coastal advancement related to sedimentary input was also recorded. Indeed, while the silty clays of unit E1 (see section 5.2) suggest quiet

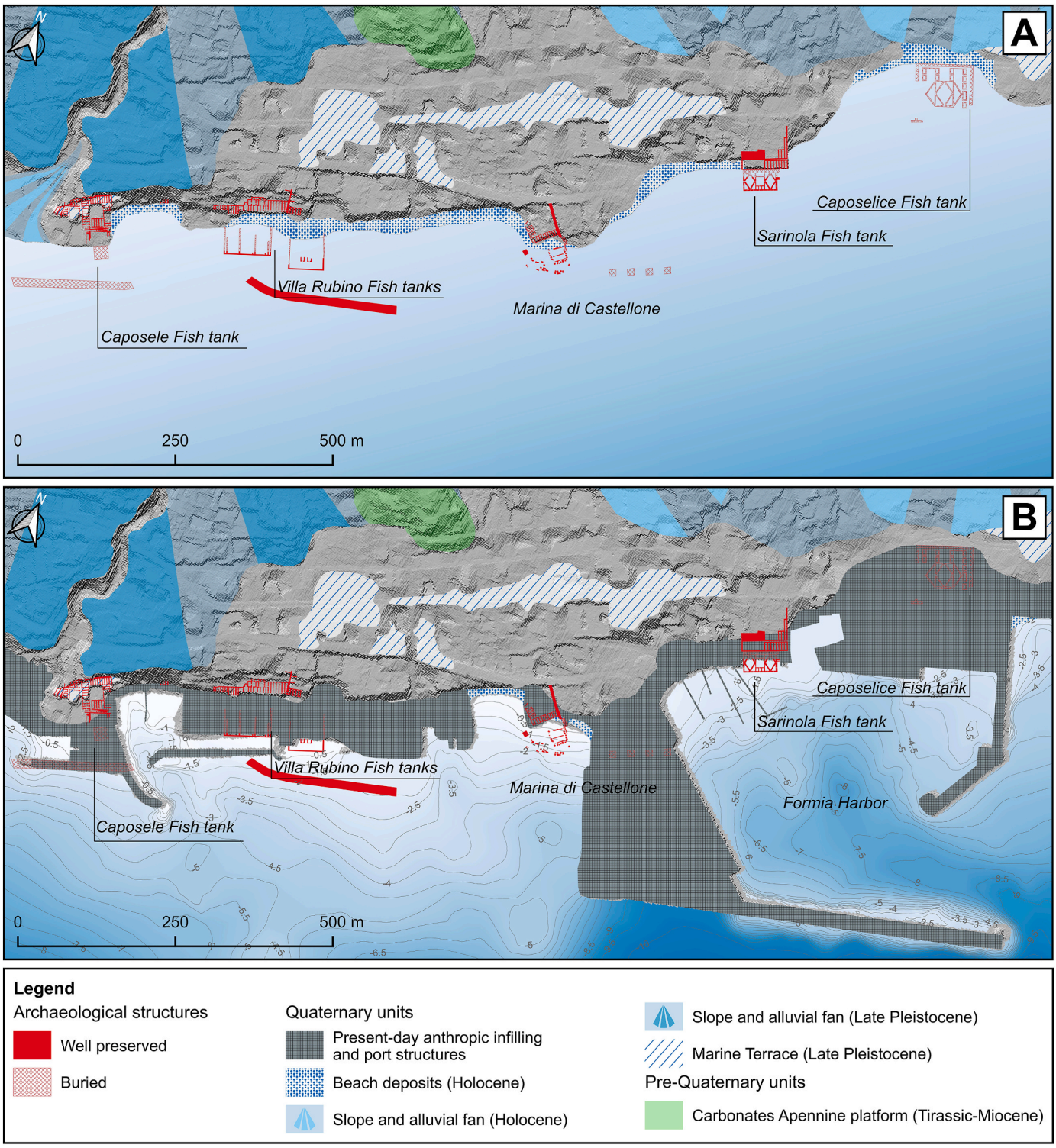

Fig. 8. – Paleoenvironmental evolution of the coastal area of Formia in the last 2 ka BP. A: morphological scenario during the Roman Period (I century BC - I century AD) with the position of the ancient archaeological structures highlighted in red; B: present-day morphology of the coastal sector, with the modern structures partially or completely englobing the Roman ones.

depositional conditions with minimal energy inputs indicative of a lagoon environment, the granulometry and colour of the sediments of unit D (see section 5.2) indicate aeolian deposition characteristic of coastal dune environment. Upward, the paleosoil located at the top of the dune (see Fig. 3) indicates a general stabilization 1.0 ± 51 ka BP. Finally, the medium-fine-grained and well-sorted sands of unit G2 suggest the permanent establishment of a coastal backshore environment characterized by moderate energy conditions and aeolian deposition.

The same evidence of prograding trends is recorded in Vendicio plain (see Fig. 1 for location), west of Formia, where the erosional transition between the volcanic unit of Cl and the silty sand of unit G1 (see Fig. 4) suggest high-energy events that reflect a fluvial environment. Unit G1 exhibits two clear transitions to blackish peaty clay (see section 5.2), characterized by planar and horizontal structure and suggesting quiet

depositional conditions and minimal energy input, indicative of temporary marsh environment transitions.

Regarding the more anthropized sector between Formia and Gaeta, the presence of fish tanks, villas and ports allowed establishing that a centimetric change in SL rise (about 0.5 m) did not influence the shoreline movements in the last 2.0 ka (Fig. 6a), which resulted in about 150 m of coastal progradation mainly due to anthropogenic forcing. In fact, the narrow beaches bordering the seacliffs that were interplayed with the coastal structures of the Roman maritime villas (Fig. 8a), disappear in the present-day scenario (Fig. 8b). The recent strong anthropization, featured by the construction of the port and various infrastructures that have partially covered and incorporated the ancient Roman structures, is the primary responsible for the coastal progradation and the total stabilization of the coastline.

7. Concluding remarks

The present work, by collecting data from various adjacent coastal sectors, has significantly advanced our understanding of Relative Sea Level (RSL) variation and the evolution of the coastal landscape in this central Mediterranean sector. So far, these aspects have been analyzed within studies referring only to the evolution of small embayment or single coastal plains, sometimes in disagreement with each other or outdated.

In this research, based on the collection of data derived from direct geoarchaeological measurements, stratigraphic and palaeoecological interpretations of new borehole data, and reinterpreting bibliographic information, two types of statistical procedures were applied. The first procedure, based on the determination of VDs through Monte Carlo simulations, takes into account the comparison between GIA models and RSL data collected within the sea proxy geodatabase. The second, based on Bayesian inference on historical rates of sea-level change and the application of the EIV IGP Model, exclusively takes into account the RSL data collected so far. In both cases, extremely small data variability was observed, always falling within the error range associated with the glacio-hydro-isostatic signal.

The study, thanks to the precise calculation of VD rates, showed that since the mid-Holocene the study area has been characterized by the absence of tectonic movements, confirming its stability. Consequently, these data can serve as a reference record for future studies of RSL variations in the western Mediterranean area, showing how sea level changed net of ground motions.

Data availability

Data available within the article and its supplementary materials.

CRediT authorship contribution statement

C. Caporizzo: Writing – original draft, Visualization, Validation, Software, Methodology, Investigation, Formal analysis, Data curation, Conceptualization. **A. Gionta:** Visualization, Methodology, Investigation, Data curation. **G. Mattei:** Writing – original draft, Visualization, Supervision, Software, Methodology, Investigation, Formal analysis, Data curation, Conceptualization. **M. Vacchi:** Writing – original draft, Visualization, Validation, Supervision, Methodology, Formal analysis, Data curation, Conceptualization. **G. Aiello:** Writing – original draft, Methodology, Data curation. **D. Barra:** Writing – original draft, Validation, Methodology, Data curation, Conceptualization. **R. Parisi:** Writing – original draft, Methodology, Data curation. **G. Corrado:** Methodology, Data curation. **G. Pappone:** Validation, Supervision, Conceptualization. **P.P.C. Aucelli:** Writing – original draft, Validation, Supervision, Funding acquisition, Formal analysis, Data curation, Conceptualization.

Declaration of competing interest

The authors declare that they have no known competing financial interests or personal relationships that could have appeared to influence the work reported in this paper.

Acknowledgements

This study received funding from the European Union - Next-GenerationEU - National Recovery and Resilience Plan (NRRP) – MISSION 4 COMPONENT 2, INVESTIMENT N. 1.1, CALL PRIN 2022 D.D. 104 02-02-2022 – PRIN_2022ZSMRXJ "GAIA project- Geomorphological and hydrogeological vulnerability of Italian coastal areas in response to sea level rise and marine extreme events CUP I53D23002130006.

This paper also benefited from the discussion at the meetings of the AIGeo (Associazione Italiana di Geografia Fisica e Gemorfologia) Working Group of Morfodinamica Costiera (2019–2023) and the discussion at the Onsea meetings (INQUA CMP project 2404).

Appendix A. Supplementary data

Supplementary data to this article can be found online at https://doi.org/10.1016/j.quaint.2024.08.009.

References

Abate, O., De Pippo, T., Ilardi, M., Pennetta, M., 1998. Studio delle caratteristiche morfoevolutive quaternarie della piana del Garigliano | The quaternary morpho-evolutionary characteristics of the Garigliano river plain (central-southern Italy). Alpine and Mediterranean Quaternary 11, 149–158.

Acocella, V., Funiciello, R., 2006. Transverse systems along the extensional Tyrrhenian margin of central Italy and their influence on volcanism. Tectonics 25. https://doi.org/10.1029/2005TC001845.

Adloff, F., Somot, S., Sevault, F., Jordà, G., Aznar, R., Déqué, M., Herrmann, M., Marcos, M., Dubois, C., Padorno, E., Alvarez-Fanjul, E., Gomis, D., 2015. Mediterranean Sea response to climate change in an ensemble of twenty first century scenarios. Clim. Dynam. 45, 2775–2802. https://doi.org/10.1007/s00382-015-2507-3.

Aiello, G., Barra, D., 2010. Crustacea ostracoda. Biol. Mar. Mediterr. 17, 401–419.

Aiello, G., Barra, D., 2011. Analisi paleoambientali attraverso microfossili calcarei. In: Pellegrino, C., R, A. (Eds.), Pontecagnano I.1 Città e Campagna Nell'Agro Picentino (Gli Scavi Dell'autostrada 2001 – 2006). Edizioni Luì, Siena, pp. 255–262.

Aiello, G., Barra, D., De Pippo, T., Donadio, C., Miele, P., Russo Ermolli, E., 2007. Morphological and palaeoenvironmental evolution of the Vendicio coastal plain in the Holocene (Latium, Central Italy). Alpine and Mediterranean Quaternary 20, 185–194.

Aiello, G., Barra, D., Collina, C., Piperno, M., Guidi, A., Stanislao, C., Saracino, M., Donadio, C., 2018. Geomorphological and paleoenvironmental evolution in the prehistoric framework of the coastland of Mondragone, southern Italy. Quat. Int. 493, 70–85. https://doi.org/10.1016/j.quaint.2018.06.041.

Aiello, G., Amato, V., Aucelli, P.P.C., Barra, D., Corrado, G., Di Leo, P., Di Lorenzo, H., Jicha, B., Pappone, G., Parisi, R., Petrosino, P., Russo Ermolli, E., Schiattarella, M., 2021. Multiproxy study of cores from the Garigliano Plain: an insight into the late quaternary coastal evolution of central-southern Italy. Palaeogeogr. Palaeoclimatol. Palaeoecol. 567 https://doi.org/10.1016/j.palaeo.2021.110298.

Amato, V., Aucelli, P.P.C., Mattei, G., Pennetta, M., Rizzo, A., Rosskopf, C.M., Schiattarella, M., 2018. A geodatabase of late Pleistocene - holocene palaeo sea-level markers in the gulf of naples. Alpine and Mediterranean Quaternary 31, 5–10.

Amorosi, A., Ricci Lucchi, M., Rossi, V., Sarti, G., 2009. Climate change signature of small-scale parasequences from Lateglacial–Holocene transgressive deposits of the Arno valley fill. Palaeogeogr. Palaeoclimatol. Palaeoecol. 273, 142–152. https://doi.org/10.1016/J.PALAEO.2008.12.010.

Amorosi, A., Rossi, V., Vella, C., 2013. Stepwise post-glacial transgression in the Rhône Delta area as revealed by high-resolution core data. Palaeogeogr. Palaeoclimatol. Palaeoecol. 374, 314–326. https://doi.org/10.1016/j.palaeo.2013.02.005.

Anthony, E.J., Marriner, N., Morhange, C., 2014. Human influence and the changing geomorphology of Mediterranean deltas and coasts over the last 6000 years: from progradation to destruction phase? Earth Sci. Rev. 139, 336–361. https://doi.org/10.1016/J.EARSCIREV.2014.10.003.

Antonioli, F., 1991. Geomorfologia subacquea e costiera del litorale compreso tra Punta Stendardo e Torre S. Agostino (Gaeta) |Subaqueous and subaerial geomorphology of the coast between Punta Stendardo and Torre S. Agostino (Gaeta, Italy). Alpine and Mediterranean Quaternary 4, 257–273.

Antonioli, F., Dai Pra, G., Hearty, P., 1988. I sedimenti Quaternari nella fascia costiera della piana di Fondi, Italia. Bollettino Società Geologia Italiana 107, 491–501. Bollettino Società Geologia Italiana 107, 491–501.

Attema, P., 2017. Sedimentation as geomorphological bias and indicator of agricultural (un)sustainability in the study of the coastal plains of South and Central Italy in

antiquity. J. Archaeol. Sci.: Report 15, 459–469. https://doi.org/10.1016/j.jasrep.2016.07.024.

Aucelli, P.P.C., Mattei, G., Caporizzo, C., Cinque, A., Troisi, S., Peluso, F., Stefanile, M., Pappone, G., 2020. Ancient coastal changes due to ground movements and human interventions in the roman portus julius (Pozzuoli Gulf, Italy): results from photogrammetric and direct surveys. Water (Switzerland) 12. https://doi.org/10.3390/W12030658.

Aucelli, P.P.C., Mattei, G., Caporizzo, C., Cinque, A., Amato, L., Stefanile, M., Pappone, G., 2021. Multi-proxy analysis of relative sea-level and paleoshoreline changes during the last 2300 years in the Campi Flegrei caldera, Southern Italy. Quat. Int. 602, 110–130. https://doi.org/10.1016/j.quaint.2021.03.039.

Aucelli, P.P.C., Mattei, G., Caporizzo, C., Di Luccio, D., Tursi, M.F., Pappone, G., 2022. Coastal vs volcanic processes: procida Island as a case of complex morpho-evolutive response. Mar. Geol. 448 https://doi.org/10.1016/j.margeo.2022.106814.

Bellotti, P., Calderoni, G., Dall'Aglio, P.L., D'Amico, C., Davoli, L., Di Bella, L., D'Orefice, M., Esu, D., Ferrari, K., Bandini Mazzanti, M., Tarragoni, C., Torri, P., 2016. Middle-to late-Holocene environmental changes in the Garigliano delta plain (Central Italy): which landscape witnessed the development of the Minturnae Roman colony? Holocene 26, 1457–1471. https://doi.org/10.1177/0959683616640055.

Bergomi, C., Catenacci, V., Cestari, G., Manfredini, M., Manganelli, V., 1969. Note illustrative della Carta Geologica d'Italia alla scala 1:100000, foglio 171 "Gaeta e vulcano di Roccamonfina.". Servizio Geologico d', Italia.

Billi, A., Bosi, V., De Meo, A., 1997. Caratterizzazione strutturale del rilievo del M. Massico nell'ambito dell'evoluzione quaternaria delle depressioni costiere dei fiumi Garigliano e Volturno (Campania Settentrionale). Il Quat. 10, 15–26.

Brancaccio, L., Cinque, A., Russo, F., Belluomini, G., Branca, M., Delitala, L., 1990. Segnalazione e datazione di depositi marini tirreniani sulla costa campana. Boll. Soc. Geol. It 109, 259–265.

Brisset, E., Burjachs, F., Ballesteros Navarro, B.J., Fernández-López de Pablo, J., 2018. Socio-ecological adaptation to Early-Holocene sea-level rise in the western Mediterranean. Global Planet. Change 169, 156–167. https://doi.org/10.1016/j.gloplacha.2018.07.016.

Budillon, F., Amodio, S., Contestabile, P., Alberico, I., Innangi, S., Molisso, F., 2020. The present-day nearshore submarine depositional terraces off the Campania coast (South-eastern Tyrrhenian Sea): an analysis of their morpho-bathymetric variability. In: MetroSea 2020 - TC19 International Workshop on Metrology for the Sea, pp. 132–138.

Budillon, F., Amodio, S., Alberico, I., Contestabile, P., Vacchi, M., Innangi, S., Molisso, F., 2022a. Present-day infralittoral prograding wedges (IPWs) in Central-Eastern Tyrrhenian Sea: critical issues and challenges to their use as geomorphological indicators of sea level. Mar. Geol. 450 https://doi.org/10.1016/j.margeo.2022.106821.

Budillon, F., Alberico, I., Amodio, S., Contestabile, P., Innangi, S., 2022b. The composite dataset of the present-day Infralittoral Prograding Wedges (IPWs) in the inner continental shelf of the Campania region (Central-Eastern Tyrrhenian Sea). Data Brief 44, 108484. https://doi.org/10.1016/J.DIB.2022.108484.

Cahill, N., Kemp, A.C., Horton, B.P., Parnell, A.C., 2015. Modeling sea-level change using errors-in-variables integrated Gaussian processes. Ann. Appl. Stat. 9, 547–571. https://doi.org/10.1214/15-AOAS824.

Caldara, M., Caroli, I., Simone, O., 2008. Holocene evolution and sea-level changes in the Battaglia basin area (eastern Gargano coast, Apulia, Italy). Quat. Int. 183, 102–114. https://doi.org/10.1016/J.QUAINT.2007.07.005.

Caporizzo, C., Aucelli, P.P.C., Di Martino, G., Mattei, G., Tonielli, R., Pappone, G., 2021a. Geomorphometric analysis of the natural and anthropogenic seascape of Naples (Italy): a high-resolution morpho-bathymetric survey. Trans. GIS 25, 2571–2595. https://doi.org/10.1111/TGIS.12829.

Caporizzo, C., Gracia, F.J., Aucelli, P.P.C., Barbero, L., Martín-Puertas, C., Lagóstena, L., Ruiz, J.A., Alonso, C., Mattei, G., Galán-Ruffoni, I., López-Ramírez, J.A., Higueras-Milena, A., 2021b. Late-Holocene evolution of the Northern Bay of Cádiz from geomorphological, stratigraphic and archaeological data. Quat. Int. 602, 92–109. https://doi.org/10.1016/j.quaint.2021.03.028.

Caporizzo, C., Gracia, F.J., Martín-Puertas, C., Mattei, G., Stocchi, P., Aucelli, P.P.C., 2024. Holocene relative sea-level variation and coastal changes in the Bay of Cádiz: new insights on the influence of local subsidence and glacial hydro-isostatic adjustments. Geomorphology 458. https://doi.org/10.1016/j.geomorph.2024.109232.

Carboni, M.G., Bergamin, L., Di Bella, L., Iamundo, F., Pugliese, N., 2002. Palaeoecological evidences from foraminifers and ostracods on Late Quaternary sea-level changes in the Ombrone river plain (central Tyrrhenian coast, Italy). Geobios 35, 40–50. https://doi.org/10.1016/S0016-6995(02)00047-5.

Carboni, M.G., Bergamin, L., Di Bella, L., Esu, D., Cerone, E.P., Antonioli, F., Verrubbi, V., 2010. Palaeoenvironmental reconstruction of late Quaternary foraminifera and molluscs from the ENEA borehole (Versilian plain, Tuscany, Italy). Quat. Res. 74, 265–276. https://doi.org/10.1016/j.yqres.2010.07.006.

Cassieri, N., 2015. Nuovi risultati di indagine dalle ville costiere formiane. Newsletter Di Archeologia (CISA) 6, 67–93.

Ciccone, S., 1992. I resti archeologici sul litorale di Formia. In: WWF - Atti del III° Seminario Internazionale di Studi sull'Ecosistema Marino. Ecosistema Marino in Italia e Sulla Costa Laziale. Formia.

Ciccone, S., 1995. Segni di un antico paesaggio marino nella Villa di Tiberio. In: WWF - Atti del IV° Seminario Internazionale di Studi sull'Ecosistema Marino. Ecosistema Marino in Italia e Sulla Costa Laziale. Formia.

Ciccone, S., 2000. Villae e piscinae del litorale formiano tra utilitas e venustas. In: Romano, E. (Ed.), Formia Romana. Storia Illustrata Di Formia. Elio Sellino Editore, Pratola Serra (AV), pp. 163–186.

Colombaroli, D., Marchetto, A., Tinner, W., 2007. Long-term interactions between Mediterranean climate, vegetation and fire regime at Lago di Massaciuccoli (Tuscany, Italy). J. Ecol. 95, 755–770. https://doi.org/10.1111/j.1365-2745.2007.01240.x.

Conti, A., Bigi, S., Cuffaro, M., Doglioni, C., Scrocca, D., Muccini, F., Cocchi, L., Ligi, M., Bortoluzzi, G., 2017. Transfer zones in an oblique back-arc basin setting: insights from the Latium-Campania segmented margin (Tyrrhenian Sea). Tectonics 36, 78–107. https://doi.org/10.1002/2016TC004198.

Corrado, G., Amodio, S., Aucelli, P.P.C., Incontri, P., Pappone, G., Schiattarella, M., 2018. Late quaternary geology and morphoevolution of the Volturno coastal plain, southern Italy. Alpine and Mediterranean Quaternary 31, 23–26.

Corrado, G., Amodio, S., Aucelli, P.P.C., Pappone, G., Schiattarella, M., 2020. The subsurface geology and landscape evolution of the Volturno coastal plain, Italy: interplay between tectonics and sea-level changes during the quaternary. Water (Switzerland) 12. https://doi.org/10.3390/w12123386.

Corrado, G., Donadio, C., Pennetta, M., Schiattarella, M., Valente, A., 2022. Pliocene to Quaternary morphotectonic evolution of the Gaeta Bay, Tyrrhenian coastal belt, central Italy: a review. Quat. Int. 638–639, 111–121. https://doi.org/10.1016/j.quaint.2022.05.010.

Cosentino, D., Federici, I., Cipollari, P., Gliozzi, E., 2006. Environments and tectonic instability in central Italy (Garigliano Basin) during the late Messinian Lago-Mare episode: new data from the onshore Mondragone 1 well. Sediment. Geol. 188–189, 297–317. https://doi.org/10.1016/j.sedgeo.2006.03.010.

De Pippo, T., Donadio, C., Miele, P., Valente, A., 2007. Morphological evidence for late quaternary tectonic activity along the coast of Gaeta (Central Italy). Geogr. Fis. Din. Quaternaria 30, 43–53.

Devoti, S., Antonioli, F., Luisa, B., Marco Fulvio, N., Sergio, S., 2004. 40-ky history of sea-level oscillations from marine and lagoonal fossils in a core from Fondi Plain (Italy). Quat. Nova 8, 213–228.

Di Lorenzo, H., Aucelli, P., Corrado, G., De Iorio, M., Schiattarella, M., Russo Ermolli, E., 2021. Environmental evolution and anthropogenic forcing in the Garigliano coastal plain (Italy) during the Holocene. Holocene 31, 1089–1099. https://doi.org/10.1177/09596836211003242.

Di Rita, F., Celant, A., Magri, D., 2010. Holocene environmental instability in the wetland north of the Tiber delta (Rome, Italy): sea-lake-man interactions. J. Paleolimnol. 44, 51–67. https://doi.org/10.1007/s10933-009-9385-9.

Di Rita, F., Simone, O., Caldara, M., Gehrels, W.R., Magri, D., 2011. Holocene environmental changes in the coastal Tavoliere Plain (Apulia, southern Italy): a multiproxy approach. Palaeogeogr. Palaeoclimatol. Palaeoecol. 310, 139–151. https://doi.org/10.1016/J.PALAEO.2011.06.012.

Doorenbosch, M., Field, M.H., 2019. A Bronze Age palaeoenvironmental reconstruction from the Fondi basin, southern Lazio, central Italy. Quat. Int. 499, 221–230. https://doi.org/10.1016/j.quaint.2018.03.022.

Eckhardt, R., 1987. Stan ulam, john von neumann, and the monte carlo method. Los Alamos Sci. 15, 131–136.

Evelpidou, N., Pirazzoli, P., Vassilopoulos, A., Spada, G., Ruggieri, G., Tomasin, A., 2012. Late holocene sea level reconstructions based on observations of roman fish tanks, Tyrrhenian coast of Italy. Geoarchaeology 27, 259–277. https://doi.org/10.1002/GEA.21387.

Fagerstrom, J.A., 1964. Fossil communities in paleoecology: their recognition and significance. GSA Bulletin 75, 1197–1216. https://doi.org/10.1130/0016-7606(1964)75[1197:FCIPTR]2.0.CO;2.

Farrell, W.E., Clark, J.A., 1976. On postglacial Sea Level. Geophys. J. Roy. Astron. Soc. 46, 647–667. https://doi.org/10.1111/j.1365-246X.1976.tb01252.x.

Fuhrmann, R., 2012. Atlas quartärer und rezenter Ostrakoden Mitteldeutschlands. Naturkundliches Museum Mauritianum.Altenburg, Altenburg, pp. 1–320. Vol. 15. vol 97/8.

Georgiou, N., Geraga, M., Francis-Allouche, M., Christodoulou, D., Stocchi, P., Fakiris, E., Dimas, X., Zoura, D., Iatrou, M., Papatheodorou, G., 2022. Late Pleistocene submarine terraces in the Eastern Mediterranean, central Lebanon, Byblos: revealing their formation time frame through modeling. Quat. Int. 638–639, 180–196. https://doi.org/10.1016/J.QUAINT.2021.12.008.

Gravina, M.F., Ardizzone, G.D., Scaletta, F., Chimenz, C., 1989. Descriptive analysis and classification of benthic communities in some mediterranean coastal lagoons (Central Italy). Mar. Ecol. 10, 141–166. https://doi.org/10.1111/j.1439-0485.1989.tb00071.x.

Heaton, T.J., Köhler, P., Butzin, M., Bard, E., Reimer, R.W., Austin, W.E.N., Bronk Ramsey, C., Grootes, P.M., Hughen, K.A., Kromer, B., Reimer, P.J., Adkins, J., Burke, A., Cook, M.S., Olsen, J., Skinner, L.C., 2020. Marine 20—the marine radiocarbon age calibration curve (0–55,000 cal BP). Radiocarbon 62, 779–820. https://doi.org/10.1017/RDC.2020.68.

Hijma, M.P., Engelhart, S.E., Törnqvist, T.E., Horton, B.P., Hu, P., Hill, D.F., 2015. A Protocol for a Geological Sea-Level Database, Handbook of Sea-Level Research. https://doi.org/10.1002/9781118452547.ch34.

Horton, B.P., Shennan, I., 2009. Compaction of Holocene strata and the implications for relative sealevel change on the east coast of England. Geology 37, 1083–1086. https://doi.org/10.1130/G30042A.1.

Iannace, P., Milia, A., Torrente, M.M., 2013. 4D geologic evolution in the Gaeta bay sedimentary infill (eastern Tyrrhenian Sea). Geoacta 12, 25–36.

Ippolito, F., Ortolani, F., Russo, M., 1973. Struttura marginale tirrenica dell'Appennino campano: reinterpretazione di dati di antiche ricerche di idrocarburi, vol. 12. Memorie Società Geologica Italiana, pp. 227–249.

Kaniewski, D., Van Campo, E., Morhange, C., Guiot, J., Zviely, D., Shaked, I., Otto, T., Artzy, M., 2013. Early urban impact on Mediterranean coastal environments. Sci. Rep. 3, 3540. https://doi.org/10.1038/srep03540.

Karkani, A., Evelpidou, N., Giaime, M., Marriner, N., Morhange, C., Spada, G., 2019. Late Holocene seasea-level evolution of paros island (cyclades, Greece). Quat. Int. 500, 139–146. https://doi.org/10.1016/j.quaint.2019.02.027.

Karymbalis, E., Tsanakas, K., Cundy, A., Iliopoulos, G., Papadopoulou, P., Protopappas, D., Gaki-Papanastassiou, K., Papanastassiou, D., Batzakis, D.V., Kotinas, V., Maroukian, H., 2022. Late holocene palaeogeographic evolution of the lihoura coastal plain, pteleos gulf, Central Greece. Quat. Int. 638–639, 70–83. https://doi.org/10.1016/J.QUAINT.2021.12.007.

Khan, N.S., Horton, B.P., Engelhart, S., Rovere, A., Vacchi, M., Ashe, E.L., Törnqvist, T.E., Dutton, A., Hijma, M.P., Shennan, I., 2019. Inception of a global atlas of sea levels since the Last Glacial Maximum. Quat. Sci. Rev. 220, 359–371. https://doi.org/10.1016/j.quascirev.2019.07.016.

Lambeck, K., Anzidei, M., Antonioli, F., Benini, A., Esposito, A., 2004. Sea level in Roman time in the Central Mediterranean and implications for recent change. Earth Planet Sci. Lett. 224, 563–575. https://doi.org/10.1016/j.epsl.2004.05.031.

Lambeck, K., Antonioli, F., Anzidei, M., Ferranti, L., Leoni, G., Scicchitano, G., Silenzi, S., 2011. Sea level change along the Italian coast during the Holocene and projections for the future. Quat. Int. 232, 250–257. https://doi.org/10.1016/j.quaint.2010.04.026.

Lambeck, K., Rouby, H., Purcell, A., Sun, Y., Sambridge, M., 2014. Sea level and global ice volumes from the last glacial maximum to the holocene. Proc. Natl. Acad. Sci. U. S.A. 111, 15296–15303. https://doi.org/10.1073/pnas.1411762111.

Leoni, G., Dai Pra, G., 1997. Variazioni del livello del mare nel tardo Olocene (ultimi 2500 anni) lungo la costa del Lazio in base ad indicatori geo-archeologici. Interazioni fra neotettonica. eustatismo e clima 1–134. ENEA, Unità comunicazione e informazioneRoma.

Marco-Barba, J., Holmes, J.A., Mesquita-Joanes, F., Miracle, M.R., 2013. The influence of climate and sea-level change on the Holocene evolution of a Mediterranean coastal lagoon: evidence from ostracod palaeoecology and geochemistry. Geobios 46, 409–421. https://doi.org/10.1016/j.geobios.2013.05.003.

Martínez-Sánchez, A., Gracia, F.J., Alonso, C., Mata, E., Caporizzo, C., 2023. Reconstructing the historical shoreline evolution of the Northern Bay of Cádiz (SW Spain) from geomorphological and geoarchaeological data. J. Maps 19, 2206585. https://doi.org/10.1080/17445647.2023.2206585.

Mattei, G., Vacchi, M., 2023. Geographic variability of the millennial sea-level changes along the coasts of Italy. Alpine and Mediterranean Quaternary 36, 1–12. https://doi.org/10.26382/AMQ.2023.01.

Mattei, G., Troisi, S., Aucelli, P.P.C., Pappone, G., Peluso, F., Stefanile, M., 2018. Sensing the submerged landscape of Nisida Roman harbour in the gulf of Naples from integrated measurements on a USV. Water (Switzerland) 10. https://doi.org/10.3390/W10111686.

Mattei, G., Caporizzo, C., Novak, A., Ronchi, L., Seeliger, M., 2022a. Lost landscapes: reconstructing the evolution of coastal areas since the late Pleistocene. Quat. Int. 638–639, 1–4. https://doi.org/10.1016/J.QUAINT.2022.09.006.

Mattei, G., Caporizzo, C., Corrado, G., Vacchi, M., Stocchi, P., Pappone, G., Schiattarella, M., Aucelli, P.P.C., 2022b. On the influence of vertical ground movements on Late-Quaternary sea-level records. A comprehensive assessment along the mid-Tyrrhenian coast of Italy (Mediterranean Sea). Quat. Sci. Rev. 279 https://doi.org/10.1016/j.quascirev.2022.107384.

Mattei, G., Amato, L., Caporizzo, C., Cinque, A., Pappone, G., Sorrentino, A., Stocchi, P., Troisi, S., Aucelli, P., 2023a. Multi-technique surveys and GIS analysis for the Roman palaeo-landscape reconstruction of Campi Flegrei volcanic area. In: 2023 IEEE International Workshop on Metrology for the Sea; Learning to Measure Sea Health Parameters, MetroSea 2023 - Proceedings, pp. 164–169. https://doi.org/10.1109/MetroSea58055.2023.10317483.

Mattei, G., Amato, L., Caporizzo, C., Cinque, A., Pappone, G., Sorrentino, A., Stocchi, P., Troisi, S., Aucelli, P.P.C., 2023b. Reconstructing anthropic coastal landscape of Campi Flegrei volcanic area (Southern Italy) during the Roman period from multi-technique surveys. J. Maps 19. https://doi.org/10.1080/17445647.2023.2187320.

Mattei, G., Caporizzo, C., Cinque, A., Pappone, G., Sorrentino, A., Troisi, S., Aucelli, P.P.C., 2024. Historical vertical ground movements in the Campi Flegrei volcano: a new transect across the caldera rim. Geomorphology 446, 108997. https://doi.org/10.1016/J.GEOMORPH.2023.108997.

Mazzini, I., Anadon, P., Barbieri, M., Castorina, F., Ferreli, L., Gliozzi, E., Mola, M., Vittori, E., 1999. Late Quaternary sea-level changes along the Tyrrhenian coast near Orbetello (Tuscany, central Italy): palaeoenvironmental reconstruction using ostracods. Mar. Micropaleontol. 37, 289–311. https://doi.org/10.1016/S0377-8398(99)00023-7.

Meisch, C., 2000. Freshwater ostracoda of western and central europe. Sußwasserfauna von Mitteleuropa 8/3.

Milia, A., Torrente, M.M., Massa, B., Iannace, P., 2013. Progressive changes in rifting directions in the Campania margin (Italy): new constrain for the Tyrrhenian Sea opening. Global Planet. Change 109, 3–17. https://doi.org/10.1016/j.gloplacha.2013.07.003.

Milia, A., Iannace, P., Tesauro, M., Torrente, M.M., 2017. Upper plate deformation as marker for the Northern STEP fault of the Ionian slab (Tyrrhenian Sea, central Mediterranean). Tectonophysics 710–711, 127–148. https://doi.org/10.1016/j.tecto.2016.08.017.

Milker, Y., Schmiedl, G., 2012. A Taxonomic Guide to Modern Benthic Shelf Foraminifera of the Western Mediterranean Sea.

Milli, S., D'Ambrogi, C., Bellotti, P., Calderoni, G., Carboni, M.G., Celant, A., Di Bella, L., Di Rita, F., Frezza, V., Magri, D., Pichezzi, R.M., Ricci, V., 2013. The transition from wave-dominated estuary to wave-dominated delta: the Late Quaternary stratigraphic architecture of Tiber River deltaic succession (Italy). Sediment. Geol. 284–285, 159–180. https://doi.org/10.1016/j.sedgeo.2012.12.003.

Milne, G.A., Mitrovica, J.X., 2008. Searching for eustasy in deglacial sea-level histories. Quat. Sci. Rev. 27, 2292–2302. https://doi.org/10.1016/J.QUASCIREV.2008.08.018.

Ozer, A., Demoulin, A., Dai Pra, G., 1987. Les indices morphologiques temoins de la stabilite tectonique de la bordure littoral du Lazio meridional (Italie). Zeitschrift fur Geomorphologie. Supplement 63, 103–117.

Peltier, W.R., 2004. Global glacial isostasy and the surface of the ice-age earth: the ICE-5G (VM2) model and GRACE. Annu. Rev. Earth Planet Sci. https://doi.org/10.1146/annurev.earth.32.082503.144359.

Pesando, F., Stefanile, M., 2015. La Villa Marittima di Gianola. Prime ricognizioni subacquee dell'Orientale di Napoli. Newsletter Di Archeologia (CISA) 6, 43–64.

Reimer, P.J., Austin, W.E.N., Bard, E., Bayliss, A., Blackwell, P.G., Bronk Ramsey, C., Butzin, M., Cheng, H., Edwards, R.L., Friedrich, M., Sookdeo, A., Talamo, S., 2020. The IntCal20 northern hemisphere radiocarbon age calibration curve (0-55 cal kBP). Radiocarbon 62, 725–757. https://doi.org/10.1017/RDC.2020.41.

Rossi, V., Amorosi, A., Sarti, G., Potenza, M., 2011. Influence of inherited topography on the Holocene sedimentary evolution of coastal systems: an example from Arno coastal plain (Tuscany, Italy). Geomorphology 135, 117–128. https://doi.org/10.1016/j.geomorph.2011.08.009.

Rovere, A., Raymo, M.E., Vacchi, M., Lorscheid, T., Stocchi, P., Gómez-Pujol, L., Harris, D.L., Casella, E., O'Leary, M.J., Hearty, P.J., 2016. The analysis of Last Interglacial (MIS 5e) relative sea-level indicators: Reconstructing sea-level in a warmer world. Earth Sci. Rev. 159, 404–427. https://doi.org/10.1016/j.earscirev.2016.06.006.

Schmiedt, G., 1972. Il livello antico del Mar Tirreno: testimonianze dei resti archeologici. Firenze.

Scicchitano, G., Spampinato, C.R., Ferranti, L., Antonioli, F., Monaco, C., Capano, M., Lubritto, C., 2011. Uplifted holocene shorelines at capo milazzo (NE sicily, Italy): evidence of co-seismic and steady-state deformation. Quat. Int. 232, 201–213. https://doi.org/10.1016/J.QUAINT.2010.06.028.

Serandrei-Barbero, R., Albani, A., Donnici, S., Rizzetto, F., 2006. Past and recent sedimentation rates in the lagoon of venice (northern Italy). Estuar. Coast Shelf Sci. 69, 255–269. https://doi.org/10.1016/J.ECSS.2006.04.018.

Sevink, J., 2020. Burnt clay or terra bruciata in coastal basins of Southern Lazio, Italy: evidence for prehistoric ignicoltura or resulting from drainage of Holocene pyritic sediments? J. Archaeol. Sci.: Report 32. https://doi.org/10.1016/J.JASREP.2020.102432.

Sevink, J., van Gorp, W., Di Vito, M.A., Arienzo, I., 2020. Distal tephra from campanian eruptions in early late holocene fills of the agro pontino graben and Fondi basin (southern lazio, Italy). J. Volcanol. Geoth. Res. 405 https://doi.org/10.1016/J.JVOLGEORES.2020.107041.

Sevink, J., Bakels, C.C., van Hall, R.L., Dee, M.W., 2021. Radiocarbon dating distal tephra from the Early Bronze Age Avellino eruption (EU-5) in the coastal basins of southern Lazio (Italy): uncertainties, results, and implications for dating distal tephra. Quat. Geochronol. 63, 101154 https://doi.org/10.1016/J.QUAGEO.2021.101154.

Shennan, I., Horton, B., 2002. Holocene land- and sea-level changes in Great Britain. J. Quat. Sci. 17, 511–526. https://doi.org/10.1002/JQS.710.

Shennan, I., Long, A.J., Horton, B.P., 2015. Handbook of seasea-level research. Handbook of Sea-Level Research, pp. 1–581. https://doi.org/10.1002/9781118452547.

Silvestri, S., Defina, A., Marani, M., 2005. Tidal regime, salinity and salt marsh plant zonation. Estuar. Coast Shelf Sci. 62, 119–130. https://doi.org/10.1016/J.ECSS.2004.08.010.

Smeraglia, L., Aldega, L., Billi, A., Carminati, E., Di Fiore, F., Gerdes, A., Albert, R., Rossetti, F., Vignaroli, G., 2019. Development of an intrawedge tectonic mélange by out-of-sequence thrusting, buttressing, and intraformational rheological contrast, Mt. Massico ridge, apennines, Italy. Tectonics 38, 1223–1249. https://doi.org/10.1029/2018TC005243.

Spada, G., Stocchi, P., 2007. SELEN: a Fortran 90 program for solving the "sea-level equation.". Comput. Geosci. 33, 538–562. https://doi.org/10.1016/j.cageo.2006.08.006.

Stocchi, P., Vacchi, M., Lorscheid, T., de Boer, B., Simms, A.R., van de Wal, R.S.W., Vermeersen, B.L.A., Pappalardo, M., Rovere, A., 2018. MIS 5e relative sea-level changes in the Mediterranean Sea: Contribution of isostatic disequilibrium. Quat. Sci. Rev. 185, 122–134. https://doi.org/10.1016/j.quascirev.2018.01.004.

Stuiver, M., Reimer, P.J., 1993. CALIB rev. 8. Radiocarbon 35, 215–230. https://doi.org/10.1017/S0033822200013904.

Tavani, S., Cardello, G.L., Vignaroli, G., Balsamo, F., Parente, M., Sabbatino, M., Raffi, I., Billi, A., Carminati, E., 2021. Segmentation of the apenninic margin of the tyrrhenian back-arc basin forced by the subduction of an inherited transform system. Tectonics 40. https://doi.org/10.1029/2021TC006770.

Traina, G., 2000. La città romana. In: Romano, E. (Ed.), Formia Romana. Storia Illustrata Di Formia. Elio Sellino Editore, Pratola Serra (AV), pp. 69–82.

Tursi, M.F., Amodio, A.M., Caporizzo, C., Del Pizzo, S., Figliomeni, F.G., Mattei, G., Parente, C., Rosskopf, C.M., Aucelli, P.P.C., 2023. The response of sandstone sea cliffs to Holocene seasea-level rise by means of remote sensing and direct surveys: the case study of Punta licosa promontory (southern Italy). Geosciences 13. https://doi.org/10.3390/GEOSCIENCES13040120.

Vacchi, M., Marriner, N., Morhange, C., Spada, G., Fontana, A., Rovere, A., 2016. Multiproxy assessment of Holocene relative sea-level changes in the western Mediterranean: sea-level variability and improvements in the definition of the isostatic signal. Earth Sci. Rev. 155, 172–197. https://doi.org/10.1016/j.earscirev.2016.02.002.

Vacchi, M., Ghilardi, M., Melis, R.T., Spada, G., Giaime, M., Marriner, N., Lorscheid, T., Morhange, C., Burjachs, F., Rovere, A., 2018. New relative sea-level insights into the

isostatic history of the Western Mediterranean. Quat. Sci. Rev. 201, 396–408. https://doi.org/10.1016/j.quascirev.2018.10.025.

Vacchi, M., Russo Ermolli, E., Morhange, C., Ruello, M.R., Di Donato, V., Di Vito, M.A., Giampaola, D., Carsana, V., Liuzza, V., Cinque, A., Boetto, G., Poveda, P., Boenzi, G., Marriner, N., 2020. Millennial variability of rates of sea-level rise in the ancient harbour of Naples (Italy, western Mediterranean Sea). Quat. Res. 93, 284–298. https://doi.org/10.1017/QUA.2019.60.

Vacchi, M., Joyse, K.M., Kopp, R.E., Marriner, N., Kaniewski, D., Rovere, A., 2021. Climate pacing of millennial sea-level change variability in the central and western Mediterranean. Nat. Commun. 12 https://doi.org/10.1038/s41467-021-24250-1.

Valente, A., 2010. Viaggio lungo la costa laziale meridionale tra sentimenti ancestrali ed emozioni del presente. In: Persi, P. (Ed.), Territoriemotivi/Geografie Emozionali. Genti e Luoghi: Sensi, Sentimenti Ed Emozioni,Atti Del V Convegno Internazionale Beni Culturali Territoriali. Dipartimento di Psicologia e del Territorio - Università degli Studi "Carlo Bo" di Urbino, Urbino, pp. 657–663.

van Gorp, W., Sevink, J., 2019. Distal deposits of the Avellino eruption as a marker for the detailed reconstruction of the early bronze age depositional environment in the agro pontino and Fondi basin (lazio, Italy). Quat. Int. 499, 245–257. https://doi.org/10.1016/j.quaint.2018.03.017.

Vitiello, S., 2017. Indagini, rilievi e ipotesi sulla peschiera romana sommersa di Villa Accetta a Gaeta. Newsletter Di Archeologia (CISA) 8, 173–199.